

TPC2-mediated Ca^{2+} signaling is required for the establishment of synchronized activity in developing zebrafish primary motor neurons.

Running title: TPC2 in zebrafish spinal circuit

Jeffrey J. Kelu, Sarah E. Webb, Antony Galione and Andrew L. Miller

HIGHLIGHTS

- TPC2-knockdown/out or pharmacological inhibition disrupts spinal circuit maturation
- Formation of the ipsilateral and contralateral synchrony requires TPC2/ Ca^{2+} signals
- TPC2 selectively activates IP_3R to mediate Ca^{2+} release
- MS222 treatment reduced NAADP levels in intact embryos

Title: TPC2-mediated Ca^{2+} signaling is required for the establishment of synchronized activity in developing zebrafish primary motor neurons.

Running title: TPC2 in zebrafish spinal circuit

Jeffrey J. Kelu¹, Sarah E. Webb¹, Antony Galione² and Andrew L. Miller^{*,1}

¹Division of Life Science & State Key Laboratory of Molecular Neuroscience, HKUST, Hong Kong,

²Department of Pharmacology, University of Oxford, Oxford, UK

*Correspondence: Andrew L. Miller, E-mail: almiller@ust.hk

Key Words: NAADP, TPC2, Ca^{2+} signaling, Spinal circuitry, Zebrafish, Acidic store.

ABSTRACT

During the development of the early spinal circuitry in zebrafish, spontaneous Ca^{2+} transients in the primary motor neurons (PMNs) are reported to transform from being slow and uncorrelated, to being rapid, synchronized and patterned. In this study, we demonstrated that in intact zebrafish, Ca^{2+} release via two-pore channel type 2 (TPC2) from acidic stores/endolysosomes is required for the establishment of synchronized activity in the PMNs. Using the SAIGFF213A;UAS:GCaMP7a double-transgenic zebrafish line, Ca^{2+} transients were visualized in the caudal PMNs (CaPs). TPC2 inhibition via molecular, genetic or pharmacological means attenuated the CaP Ca^{2+} transients, and decreased the ipsilateral and contralateral correlation, indicating a disruption in normal spinal circuitry maturation. Furthermore, treatment with MS222 resulted in a complete (but reversible) inhibition of the CaP Ca^{2+} transients, as well as a significant decrease in the concentration of the Ca^{2+} mobilizing messenger, nicotinic acid adenine diphosphate (NAADP) in whole embryo extract. Together, our new data suggest a novel function for NAADP/TPC2-mediated Ca^{2+} signaling in the development, coordination, and maturation of the spinal network in zebrafish embryos.

HIGHLIGHTS

- TPC2-knockdown/out or pharmacological inhibition disrupts spinal circuit maturation
- Formation of the ipsilateral and contralateral synchrony requires TPC2/ Ca^{2+} signals
- TPC2 selectively activates IP_3R to mediate Ca^{2+} release
- MS222 treatment reduced NAADP levels in intact embryos

INTRODUCTION

During early zebrafish (*Danio rerio*; Hamilton, 1822) development (i.e., starting at ~17.5 hpf), the primary motor neurons (PMNs) begin to display spontaneous and stochastic Ca^{2+} activity (Muto et al., 2011; Warp et al., 2012), which coincides with the generation of Ca^{2+} transients in the slow muscle cells (SMCs; Brennan et al., 2005) and spontaneous SMC-mediated coilings of the trunk (Saint-Amant and Drapeau, 1998). As development proceeds, this early motor behavior matures into an organized form of swimming (Naganawa and Hirata, 2011). This transition requires the establishment of a synchronized, correlated connectivity within the spinal network and with the developing cells of the myotome. A better understanding of the signaling elements that pattern the nascent nervous system will help in deciphering the complexity of adult behaviour (Wilson et al., 2002). The development of the genetically-encoded Ca^{2+} indicator, GCaMP, has greatly advanced our understanding about how the spontaneous Ca^{2+} -related activity in the neural network emerges and matures during embryogenesis (Muto et al., 2011; Akerboom et al., 2012). Indeed, using GCaMP, Ca^{2+} transients have been visualized in the PMNs from ~17 hpf to 24 hpf (Plazas et al., 2013), where those at ~17-18 hpf are slow, sporadic, and uncorrelated, and those generated at ~24 hpf are fast, ipsilaterally correlated and contralaterally anti-correlated (Muto et al., 2011). These data are also consistent with electrophysiological studies conducted with primary neurons (Saint-Amant and Drapeau, 2000; 2001).

Ca^{2+} has previously been reported to help regulate neuronal differentiation and proliferation, as well as axon growth and guidance (Rosenberg and Spitzer, 2011). Ca^{2+} can enter the cytoplasm of neurons either from the extracellular space, or from intracellular stores such as the endoplasmic reticulum (ER; Berridge, 2012), mitochondria (Rizzuto et al., 2012), and acidic stores/endolysosomes (Hui, et al., 2015). NAADP is the most potent Ca^{2+} mobilizing messenger reported to date (Galione, 2011), and it has been reported to target acidic stores to mediate Ca^{2+} release via activation of two-pore channels (TPCs; Calcraft et al., 2009; Ruas et al., 2015). TPCs are localized to acidic store compartments, and in addition to NAADP, they can also be regulated by multiple other modulators, including: Mg^{2+} , phosphatidylinositol-(3,5)-bisphosphate, and the P38 and JNK kinases (Jha et al., 2014). It has been suggested that the release of Ca^{2+} from the acidic stores via TPCs is highly localized, and that this initial release can induce (or trigger) further Ca^{2+} release from the ER via Ca^{2+} -induced Ca^{2+} release (CICR) from the ER. This indicates the presence of crosstalk between the acidic store and ER Ca^{2+} stores (Galione, 2011). Several reports describe the possible contribution of acidic stores to neuronal Ca^{2+} signaling. For example, NAADP was shown to potentiate neurite outgrowth and drive the differentiation of cultured neurons (Brailoiu et al., 2005; 2006). More recently, NAADP/TPC2 signaling was suggested to play a crucial role in the neural fate determination and differentiation of embryonic stem cells (Zhang et al., 2013). In addition, it was demonstrated in primary cultured

neurons that Ca^{2+} release from the endolysosomes triggers Ca^{2+} influx across the plasma membrane via voltage-gated Ca^{2+} channels (Hui et al., 2015). Although most of the previous work on TPC-mediated Ca^{2+} signaling in neural development has been limited to *in vitro* experiments, relatively few studies have explored its expression and function during the formation of the neural circuitry *in vivo* in an intact developing vertebrate.

We recently reported via morpholino oligonucleotide (MO)-mediated knockdown, homozygous and heterozygous knockout, or pharmacological inhibition of TPC2, that in zebrafish embryos, TPC2-mediated Ca^{2+} -release plays a key role in the differentiation, development, and early contractile activity of the trunk SMCs (Kelu et al., 2015; 2017). These events begin at ~17.5 hpf, and coincide with the spontaneous activity in the CaPs that initially innervate the pioneering SMCs (Melançon et al., 1997). As a result, the spontaneous activity in the CaPs initiates the early locomotory behavior of the developing embryo (Saint-Amant and Drapeau, 2000). Here, in order to study the Ca^{2+} release during the early development of the spinal circuitry, the SAIGFF213A;UAS:GCaMP7a double-transgenic line of fish, which expresses GCaMP7a strongly in the CaPs (Muto et al., 2011), was utilised. To explore the possible role of TPC2-mediated Ca^{2+} signaling in the CaPs, Ca^{2+} imaging was then performed at ~24 hpf following TPC2 attenuation via the three methods (knockdown, knockout and inhibition) described above. We report that disruption of TPC2 function resulted in a loss of both the ipsilateral correlation and contralateral anti-correlation of the Ca^{2+} signaling in the CaPs, initially reported by Muto et al. (2011). There was also a reduction in the frequency and amplitude of the Ca^{2+} transients recorded from the CaPs, and a concomitant increase in the duration of the CaP Ca^{2+} transients. The inhibition of action potentials with MS-222 resulted in the complete (but reversible) attenuation of the CaP Ca^{2+} transients, and also a decrease in whole-embryo NAADP levels. Together, these data suggest a novel role for TPC2-mediated Ca^{2+} signaling in the development of the spinal network required for the establishment of early coordinated locomotory behavior.

MATERIALS AND METHODS

Zebrafish husbandry and embryo collection

The AB wild-type zebrafish line, the Gal4:SAIGFF213A and UAS:GCaMP7a, UAS:GFP transgenic lines (Muto et al., 2011), and the *tpcn2^{dhkz1a}* mutant line (Kelu et al., 2017) were maintained, and their fertilized eggs collected, as previously described (Cheung et al., 2011). AB fish were obtained from the ZIRC (University of Oregon, OR, USA), and the Biomedical Services Unit, John Radcliffe Hospital (University of Oxford, UK); whereas the Gal4:SAIGFF213A, UAS:GCaMP7a, and UAS:GFP transgenic lines were provided by Koichi Kawakami (NIG, Japan). Fertilized eggs (collected from mating adult pairs aged between 6 to 12 months old), were maintained in Danieau's solution at ~28°C (Westerfield, 2000), or at room temperature (~23°C), to slow development until the desired stage was reached. All the procedures used in this study with live fish were performed in accordance with the guidelines and regulations set out by the Animal Ethics Committee of the HKUST and by the Department of Health, Hong Kong.

Design and injection of MO oligomers and mRNA rescue construct

The standard control-MO, *p53*-MO, *TPCN2*-MO-T, and mutant *tpcn2* mRNA were designed, prepared and injected into embryos as previously described (Kelu et al., 2015; 2017).

Preparation of the spinal neuron primary cell cultures

Primary cultures were prepared using a protocol modified from one used to prepare primary skeletal muscle cells from zebrafish embryos (Kelu et al., 2015). In brief, the trunks of ~18 hpf SAIGFF213A;UAS:GFP double-transgenic embryos were excised and then dissociated to obtain a single-cell suspension. Cells were plated on laminin-coated glass coverslips, to encourage the attachment and growth of dissociated spinal neurons (Andersen, 2002). Cells were cultured at ~28°C for ~24 h, after which they were fixed with phosphate buffered saline (PBS) containing 4% paraformaldehyde (Electron Microscopy Sciences, PA, USA) for 15 min at room temperature prior to immunocytochemistry.

Immunocytochemistry

Once fixed, the primary cell cultures were immunolabeled as described previously (Kelu et al., 2017), with the following primary antibodies: znp-1 (DHSB; at a 1:50 dilution), anti-LAMP1 (ab24170, Abcam; at a 1:50 dilution), anti-TPC2 (Kelu et al., 2015; at 1:10), anti-inositol 1,4,5-trisphosphate receptor (IP₃R) type I (407145, Calbiochem; at 1:10), anti-IP₃R type II (I-7654, Sigma-Aldrich; at 1:10), anti-IP₃R type III (I-7629, Sigma; at 1:250), and the 34C anti-RyR (R129, Sigma; at 1:500). The secondary

antibodies used were the Atto 647N-tagged goat anti-rabbit or goat anti-mouse IgGs (15048 and 15038, respectively, Active Motif; both at a dilution of 1:200;). The immunolabeled cells were then mounted under ProLong Gold + DAPI (P36931; Life Technologies). Some cells were incubated with secondary antibody alone to verify that the level of non-specific binding was negligible. Both the primary and secondary antibody incubation steps were conducted for 1 h at room temperature (i.e., ~23°C).

Images of the immunolabelled cells were acquired using a Leica TCS SP5 II laser scanning confocal microscope with a Leica HCX PL APO 40X/1.25-0.75 NA oil immersion objective lens. Alexa Fluor 488, Atto 647N and DAPI fluorescence was captured using 488 nm excitation/519 nm detection, 633 nm excitation/669 nm detection, and 405 nm excitation/461 nm detection, respectively.

Confocal imaging of live SAIGFF213A;UAS:GCaMP7a embryos

Confocal imaging (with the Leica microscope described above) was also used to image the Ca^{2+} transients generated by the CaPs in the developing spinal cord. Dechorionated SAIGFF213A;UAS:GCaMP7a embryos (with/without treatment) at ~18 hpf or ~24 hpf were oriented dorsal side down and then embedded in 2% low gelling temperature agarose in a glass-bottomed culture dish (MatTek) to restrict their motility. For the drug treatment experiments, bafilomycin A1, *trans*-Ned-19, IP_3/BM , caffeine, ryanodine, or MS-222 were mixed with the low gelling temperature agarose used to mount the embryos, and once the gel had set, the imaging dishes were then flooded with Danieau's solution containing the appropriate drug, to ensure constant exposure to the drugs during imaging. Series of time-lapse fluorescence images were then obtained from a dorsal view at the level of the ventral spinal cord where the CaPs are located, at ~13.33 Hz for a period of ~300 sec. The green fluorescence of GCaMP7a was captured using 488 nm excitation and 519 nm detection via a Leica HC PL APO 20X/ 0.7 NA objective lens with the pinhole fully open at 600 μm . The power of the laser was kept constant across fish and conditions, and the temperature was maintained at ~28°C throughout imaging.

To detect the GCaMP7a fluorescence generated in the CaPs, circular regions of interest (ROIs; each with an area of ~177 μm^2), were positioned on the cell bodies of three CaPs on either side of the spinal cord using ImageJ (NIH). Following the inhibition of TPC2 activity, embryos exhibited only a minimal level of motility (Kelu et al., 2017). The control embryos did move during the imaging period as a result of the spontaneous coilings that were taking place. However, we wanted to conduct these experiments in the most natural conditions possible, and therefore we did not use drugs that would inhibit the locomotory behavior of the embryos. Thus, embryos were embedded in 2% low-gel temperature agarose to minimize (but not completely inhibit) movement. In addition, during the

analysis, ROIs were located on CaPs in the more anterior regions of the trunk that exhibited minimal movement.

The peaks of GCaM7a fluorescence in the various fluorescence intensity profiles were identified by visual inspection, and the frequencies were calculated by dividing the number of peaks by the duration of imaging (i.e., ~300 sec). The amplitude was defined as the fold change in the mean fluorescence intensity of the peaks relative to the basal fluorescence (i.e., F_{\max}/F_0). The change in fluorescence (ΔF) was obtained by calculating the difference between the F_{\max} and the F_0 . To obtain the full-duration at half maximum (FDHM), Gaussian curve fitting was performed on individual GCaMP7a transients obtained from the fluorescence intensity profiles using ImageJ, as previously described (Kalu et al., 2017).

Pharmacological treatments

Stock solutions of bafilomycin A1 (160 μ M; Tocris Bioscience), *trans*-ned-19 (50 mM; Enzo Life Sciences, Inc.), IP₃/BM (10 mM; Sinova), and caffeine (10 mM; Sigma) were prepared as previously described (Kalu et al., 2017). Bafilomycin A1, *trans*-Ned-19, IP₃/BM, and caffeine were used at 1 μ M, 250 μ M, 100 μ M, and 2 mM, respectively (all diluted in Danieau's solution). Stock and working solutions of ryanodine (Sigma) were prepared at 5 mM in Milli-Q water and at 1 μ M in Danieau's solution, respectively. At 1 μ M, ryanodine acts as a RyR agonist and it therefore triggers the RyR-mediated release of Ca²⁺ (Meissner, 1986). In brief, embryos were dechorionated, and their terminal tail buds were excised just prior to the start of the drug treatment at ~17 hpf, as described previously (Kalu et al., 2017). Control embryos were incubated in Danieau's solution containing 1% DMSO alone after tail bud excision. In all cases, the embryos were treated with the drugs continuously from ~17 hpf and during data collection.

A stock solution of MS-222 (Sigma) was prepared at 0.4% in Milli-Q water and adjusted to pH 7. A working solution of ~0.02% MS-222 was then prepared in Danieau's solution just prior to use. Dechorionated embryos were embedded in low gelling temperature agarose and imaged from ~17 hpf to ~24 hpf in Danieau's solution. They were then incubated with 0.02% MS-222 from ~24 hpf to ~25 hpf, after which they were thoroughly rinsed to remove the MS-222 and imaged again from ~25 hpf to ~26 hpf.

NAADP extraction and cycling assay

Embryos at ~24 hpf were dechorionated, immersed in 1.5 M perchloric acid and sonicated on ice to extract NAADP. The removal of endogenous nucleotides and the NAADP cycling assay were then performed according to a well-established protocol (Graeff and Lee, 2013).

Statistical analysis

Numerical data were exported to Minitab 17.3.1 for statistical analysis using the following non-parametric tests (Dinno, 2015): 1) the Mann-Whitney Test (for comparison between two groups); or 2) the Kruskal-Wallis Test (for comparison between multiple groups). The latter was followed by the Dunn's post-hoc test to determine statistical significance in individual comparison pairs. $P < 0.05$ was considered to be statistically significant.

RESULTS

Effect of TPC2 knockdown (\pm mRNA rescue) and TPC2 heterozygous-knockout on the CaP Ca^{2+} transients at ~24 hpf

In the MO control embryos, Ca^{2+} transients were observed in the cell bodies of the CaPs during their spontaneous activity at ~24 hpf (Fig. 1Ai-Aiv,Bi-Biv). Moreover, these Ca^{2+} transients were generated in a synchronous, but alternating, manner on the ipsilateral and contralateral sides (compare the transients in the ROIs on the left side of the trunk, with those on the right; Fig. 1Av-Bv). When TPC2 was knocked-down using *TPCN2*-MO-T, *TPCN2*-MO-S or a combination of both these MOs, Ca^{2+} transients were still generated by the CaPs, however, the synchronicity was disrupted (Figs 1C, S1Aa, S1Ab). Thus, Ca^{2+} transients were generated in the ipsilateral CaPs with irregular intervals, but they were sometimes generated concurrently in the contralateral CaPs (Figs 1Ci-Cv, S1Aai-Abv). The defects in the CaP Ca^{2+} signaling activity observed in the TPC2 morphants could be partially rescued by overexpressing a mutant *tpcn2* mRNA not recognized by the *TPCN2*-MO-T (Kelu et al., 2015; 2017). In the rescued embryos, there was an increase both in the synchronicity of the CaP-generated ipsilateral Ca^{2+} transients on both sides of the spinal cord and in the alternation of the Ca^{2+} signals generated in the contralateral CaPs (Fig. 1Di-Dv).

We then compared the Ca^{2+} transients generated in the CaPs of embryos from SAIGFF213A;UAS:GCaMP7a fish that had intact *tpcn2* (termed *tpcn2*^{+/+}; Fig. 1E) with those from double-transgenic heterozygous mutant fish, generated by crossing the SAIGFF213A;UAS:GCaMP7a fish with the homozygous *tpcn2* mutants (i.e., *tpcn2*^{-/-}; Fig. 1F). The Ca^{2+} transients generated in the *tpcn2*^{+/+} controls were very similar to those generated by the two MO controls (compare Fig. 1E with Fig. 1A,B). However, in the *tpcn2*^{-/-} mutants, Ca^{2+} transients were generated in the CaPs on both sides of the spinal cord simultaneously (Fig. 1Fi-Fiv). The synchronicity of CaP activity was disrupted; however, the frequency of the Ca^{2+} signals appeared to be somewhat similar to the *tpcn2*^{+/+} controls (compare Fig. 1Fv-Fvi with Fig. 1Ev-Evi).

Cross correlograms (with lag ± 1.5 sec) were generated (Muto et al., 2011; Warp et al., 2012) to compare the Ca^{2+} signaling activity in two of the ipsilateral ROIs (i.e., comparing L1 with L2, or R1 with R2; Fig. 2Aai-Afi), as well as that in the ipsilateral and contralateral ROIs (i.e., comparing R1 or R2 with L1 or L2; Fig. 2Aaii-Afii) in the representative embryos from Fig.1. In all of the control embryos, the activity in the ipsilateral ROIs was positively correlated (reflecting the synchronized activity of the CaPs on the same side of the spinal cord). This is shown by the highly positive cross correlation function (CCF) at lag 0 (CCF0), i.e., ~0.7 to 0.9 (Fig. 2Aai,Abi,Aei). In contrast, the activity in the contralateral ROIs was negatively correlated (reflecting the alternating activity of the CaPs on either side of the spinal cord), which resulted in a negative CCF0, i.e., ~-0.2 to -0.4 (Fig. 2Aaii,Abii,Aeii). After TPC2-

knockdown with TPCN2-MO-T, the correlation of the activity in the ipsilateral ROIs decreased (CCF0= \sim 0.2; Fig. 2Aci). However, the correlation of the Ca²⁺ signaling activity in the contralateral ROIs increased dramatically (CCF0= \sim 0.6; Fig. 2Aci). When TPCN2-MO-T was co-injected with *tpcn2*-mRNA, the CCF0 of the Ca²⁺ signaling activity in the ipsilateral ROIs and the contralateral ROIs increased (CCF0= \sim 0.9; Fig. 2Adi) and decreased (CCF0= \sim 0.2; Fig. 2Adii), respectively, when compared with the TPC2 morphants (compare Fig. 2Ad with Fig. 2Ac). In the heterozygous *tpcn2* mutant (*tpcn2*^{+/-}), there was a slight decrease in the correlation of activity in the ipsilateral ROIs (CCF0= \sim 0.6) when compared with the *tpcn2*^{+/+} controls (CCF0= \sim 0.9; compare Fig. 2Afi with Fig. 2Aei). This was accompanied by an apparent increase in the correlation of activity in the contralateral ROIs in the *tpcn2*^{+/-} (CCF0= \sim 0.3; Fig. 2Afi) when compared with the *tpcn2*^{+/+} controls (CCF0= \sim 0.4; Fig. 2Aei).

Statistical analysis of the Ca²⁺ signaling activity in the ipsilateral CaPs (Fig. 2Ba) showed that significant differences were found between: The MO controls and the TPC2 morphant group (at $p < 0.001$); the TPC2 morphant group and the rescued group (at $p < 0.001$); and the *tpcn2*^{+/+} controls and *tpcn2*^{+/-} mutants (at $p < 0.01$; Fig. 2Ba). The decrease in the CCF0 values in the TPC2 morphants and *tpcn2*^{+/-} mutants suggests a disruption in the synchronicity in the ipsilateral CaPs whereas the increase in CCF0 in the rescued embryos suggests a partial restoration of synchronicity.

Analysis of the Ca²⁺ signaling activity in the contralateral CaPs (Fig. 2Bb) showed that significant differences were found when comparing the MO controls (negative CCF0) with the TPC2 morphants (positive CCF0), and the *tpcn2*^{+/+} controls (negative CCF0) with the *tpcn2*^{+/-} mutants (positive CCF0; both at $p < 0.001$). In addition, even though the CCF0 values of the contralateral CaP Ca²⁺ signaling activity in the TPC2 morphants and the rescued embryos were both positive, when comparing the two, the CCF0 of the latter was significantly lower (at $p < 0.05$), suggesting a partial restoration of the anti-correlation in these embryos (Fig. 2Bb).

The frequency, amplitude and duration of the Ca²⁺ transients generated in the different treatment groups were also determined (Fig. 2C-E). In the MO controls, the Ca²⁺ signals were generated at a frequency of \sim 0.17-0.18 Hz; an amplitude (F_{\max}/F_0) of \sim 14.00-15.00 AU; and a duration of \sim 1.50 s. In the TPC2 morphants, however, the frequency and amplitude of the Ca²⁺ signals were significantly lower ($p < 0.001$) than the MO controls with values of \sim 0.01 Hz and 4.00 AU, respectively. In addition, the duration of the signals was significantly longer than the MO controls ($p < 0.001$), with a value of \sim 6.00 s. In the rescue group, all the features of the signals were significantly different when compared with the morphant group (i.e., frequency at $p < 0.5$, amplitude $p < 0.01$, and duration at $p < 0.5$). The frequency, amplitude and duration of the Ca²⁺ transients generated in the *tpcn2*^{+/+} controls were similar to those generated in the MO controls. In the *tpcn2*^{+/-} mutants, however, the frequency and amplitude were significantly lower (at $p < 0.01$ and $p < 0.05$, respectively) than the *tpcn2*^{+/+} controls.

Effect of depleting the acidic Ca^{2+} stores and antagonizing TPCs on the development of the spinal neural circuitry

A pharmacological approach with bafilomycin A1 and *trans*-ned-19 was also used to support our molecular and genetic data. Bafilomycin A1 is a vacuolar H^+ -ATPase inhibitor, which depletes the acidic stores (Bowman et al., 1988), and *trans*-ned-19 is a specific antagonist of the TPCs (Naylor et al., 2009). Our results showed that in the untreated and DMSO-treated SAIGFF213A;UAS:GCaMP7a embryos, long-duration, low-frequency Ca^{2+} transients were generated at ~18 hpf (Fig. 3Ai-Av,Ci-Cv), and short-duration, high-frequency Ca^{2+} transients were generated at ~24 hpf (Fig. 3Bi-Bv,Di-Dv). Furthermore, the Ca^{2+} transients at ~24 hpf were highly synchronized in the ipsilateral CaPs, whereas in the contralateral CaPs, there was an alternating pattern of activity (Fig. 3Bi-Bv,Di-Dv).

When SAIGFF213A;UAS:GCaMP7a embryos were treated with either 1 μM bafilomycin A1 or 250 μM *trans*-ned-19 for 1 h starting at ~17 hpf, the Ca^{2+} transients imaged at ~18 hpf were (similar to the DMSO controls) of relatively long-duration and low-frequency, and there appeared to be a low correlation between the Ca^{2+} signaling activity in the ipsilateral CaPs (compare Fig. 3Ei-Ev and Fig. 3Gi-Gv with Fig. 3Ci-Cv). However, when the embryos were treated with the bafilomycin A1- or *trans*-ned-19 for 7 h, the Ca^{2+} transients generated at ~24 hpf were (unlike the DMSO controls) still similar to the long-duration and low-frequency type observed at ~18 hpf (compare Fig. 3Fi-Fv and Fig. 3Hi-Hv with 3Di-Dv). In addition, the simultaneous and alternating Ca^{2+} signaling activity observed in the ipsilateral and contralateral CaPs, respectively, in the DMSO controls, was not present in the bafilomycin A1- or *trans*-ned-19-treated embryos at ~24 hpf. Moreover, occasionally a simultaneous bi-activation of the CaPs on both sides of the spinal cord occurred (see Ca^{2+} transients within the grey bars in Figs 3Fv-Hv,Hv-Hv).

Statistical analyses showed that at ~18 hpf, the CCF0 values of the Ca^{2+} signaling activity in the ipsilateral CaPs in untreated embryos and following treatment with DMSO, bafilomycin A1- or *trans*-ned-19, were not significantly different (Fig. 4Aa). All exhibited a CCF0 of ~0.2, which suggests a low correlation of the ipsilateral Ca^{2+} signaling activity. At ~24 hpf, the CCF0 of the ipsilateral Ca^{2+} signaling activity in the untreated or DMSO-treated controls was ~0.9. In contrast, the bafilomycin A1- or *trans*-ned-19-treated embryos had a higher CCF0 than they did at ~18 hpf (i.e., ~0.4), but they were significantly lower (at $p < 0.01$ and $p < 0.001$, respectively) than those of the untreated and DMSO-treated controls (Fig. 4Aa).

In the bafilomycin A1- or *trans*-ned-19-treated embryos at ~18 hpf (Fig. 4Ab), the CCF0 values of the Ca^{2+} signaling activity in the contralateral CaPs were not significantly different from the controls, with all the groups exhibiting a low CCF0 of ~0.1, which implies a low correlation of the activity in the

contralateral CaPs at this early stage. At ~24 hpf, in the control embryos an anti-correlation (CCF0 of ~0.15) was observed in the Ca^{2+} transients generated by the contralateral CaPs. In the drug-treated embryos, however, the CCF0 (of ~0.1) was significantly higher (at $p < 0.001$; Fig. 4Ab) than that of the controls. In addition, in the bafilomycin A1- or *trans*-ned-19-treated embryos, the CCF0 values of the Ca^{2+} signaling activity in the contralateral CaPs were not significantly different, when comparing embryos at ~18 hpf and ~24 hpf (Fig. 4Ab).

The frequency, amplitude and duration of the Ca^{2+} transients generated in the various treatment groups were also determined (Fig. 4B-D). For each parameter measured, Ca^{2+} transients generated in the drug-treated embryos were not significantly different from those generated in the controls at ~18 hpf. Thus, in each treatment group, the frequency, amplitude and duration of the Ca^{2+} transients were ~0.02 Hz, ~4.00 AU and ~8.00 s, respectively. However, at ~24 hpf, the frequency and amplitude of the transients generated in the drug-treated embryos remained at the low level observed at ~18 hpf, and thus they were significantly lower than the controls (at $p < 0.001$; Fig. 4B,C). In addition, the slow duration Ca^{2+} transients observed at ~18 hpf in all groups, remained more or less unchanged in the drug-treatment groups, contrasting the significantly faster durations observed for the Ca^{2+} transients in the control groups (at $p < 0.01$ and $p < 0.001$ for the bafilomycin A1- and *trans*-ned-19-treated embryos, respectively; Fig. 4D).

Effect of stimulating the ER-mediated Ca^{2+} release in the regulation of CaP Ca^{2+} transients during spontaneous activity after TPC2-knockdown

TPC2 morphants at ~17 hpf were treated with IP_3/BM , or with caffeine or a low (agonistic) concentration of ryanodine for 7 h, and the ability of these drugs to up-regulate Ca^{2+} release from the ER at ~24 hpf was determined (Fig. 5). The results showed that in the DMSO-treated TPC2 morphants, a similar Ca^{2+} signaling phenotype was observed when compared with the TPC2 morphants cultured in the absence of DMSO (compare Fig. 5Aai-Aav with Fig. 1Ci-Cv). When TPC2 morphants were treated with IP_3/BM , the Ca^{2+} transients generated in the ipsilateral CaPs became more synchronous, and those in the contralateral CaPs showed a more alternating pattern of generation (Fig. 5Abi-Abiv). Moreover, the bi-activation of the transients (observed in the DMSO-treated TPC2 morphants) was absent (Fig. 5Abv-Abv). In contrast, when TPC2 morphants were treated with either caffeine or a low concentration of ryanodine, the MO-related defects in the Ca^{2+} signaling signature were not improved, and the simultaneous bi-activation of the CaPs on both sides of the spinal cord was observed (Fig. 5Aci-Acv, 5Adi-Adv).

These results were confirmed via statistical analysis (Fig. 5B-E). With regards to the cross correlation, the IP_3/BM -treated TPC2 morphants gave a significantly greater CCF0 (of ~0.7) for the

ipsilateral Ca^{2+} transients (at $p < 0.001$), when compared with the DMSO-treated controls ($\text{CCF0} \sim 0.2$; Fig. 5Ba). In contrast, the RyR agonists both gave a $\text{CCF0} \sim 0.2$ for the activity of the ipsilateral CaPs, and thus these were not significantly different from the DMSO controls (Fig. 5Ba). For the cross correlation of the activity of the contralateral CaPs, however, no statistical significant differences were found when comparing the various treatment groups with the control group, even though the IP_3/BM treatment showed a slightly lower CCF0 (of ~ 0.05) when compared with the others (with a $\text{CCF0} \sim 0.1$; Fig. 5Bb). In addition, the frequency and amplitude of the Ca^{2+} transients generated in the IP_3/BM treatment group alone showed a significant increase (both at $p < 0.001$), and the duration of the transients was significantly decreased (at $p < 0.01$), when compared with the DMSO treatment group (Fig. 5C-E). In contrast, the properties of the Ca^{2+} transients generated in the caffeine and low concentration ryanodine treatment groups were not significantly different from the DMSO controls (Fig. 5C-E).

To further investigate the role of ER-mediated Ca^{2+} release in the maturation of the spinal neural circuitry, SAIGFF213A;UAS:GCaMP7a embryos were treated with a SERCA inhibitor (thapsigargin), antagonists of the IP_3R (2-APB or xestospongin C), or antagonists of the RyR (dantrolene or ryanodine; Fig. S2). Our results demonstrated that treatment with the SERCA and IP_3R antagonists (but not the RyR antagonists) could mimic the inhibitory effect of MO-mediated TPC2-knockdown on the maturation of the spinal neural circuitry (compare Fig. S2 with Fig. 1C).

Expression and localization of lysosomes, TPC2, IP_3Rs and RyRs in cultured primary neurons

Primary cultures were prepared from the trunk of SAIGFF213A;UAS:GFP double-transgenic embryos at ~ 18 hpf, and then they were cultured for 24 h after which they were fixed and immunolabelled with antibodies to PMNs, lysosomes (LAMP1), TPC2, IP_3R type I-III, or the RyR (Fig. 6). In these embryos the CaPs were genetically labelled with GFP (Muto et al., 2011). This was confirmed in the primary cultures, by co-labeling with the PMN-specific antibody, znp-1 (Fig. 6Ai-Aiv). For the other immunolabelling experiments, the presumptive CaPs were identified both via the expression of GFP and via their unipolar morphology, the latter being a feature reported previously for PMNs in primary culture (Chen et al., 2013). The results showed that LAMP1 and TPC2 were both expressed in the cell bodies and the axons of the CaP-like cells (Fig. 6Bi-Biv, Ci-Civ); LAMP1 was expressed mainly in the cytoplasm of the cell body with a lower level of expression in the nucleus. In contrast, TPC2 was expressed throughout the cell body. Of the three IP_3R sub-types, IP_3R type I showed a distinct perinuclear localization in the cell body of the CaP-like cells, and it was also expressed in the axons (Fig. 6Di-Div); whereas IP_3R type II was expressed in the cell body but not in the axons (Fig. 6Ei-Eiv). In contrast, no IP_3R type III expression was seen in either the cell body or axons of these cells (Fig. 6Fi-

Fiv). The 34C antibody, which according to the manufacturer can detect RyR types I-III was also used, but no RyR expression was detected in the CaP-like cells (Fig. 6Gi-Giv). A secondary antibody control was used to demonstrate the negligible level of non-specific secondary antibody labeling (Fig. 6H).

Effect of MS222 on the CaP-generated Ca^{2+} transients, and synthesis of NAADP in intact zebrafish embryos

SAIGFF213A;UAS:GCaMP7a embryos were imaged at ~24 hpf. They were then treated with MS-222 (~0.02%) for 1 h before being imaged again at ~25 hpf. The MS-222-treated embryos were then rinsed with Danieau's solution for 1 h before being imaged once again at ~26 hpf (Fig. 7A). At ~24 hpf (Fig. 7Aa), the Ca^{2+} transients generated were similar in frequency and amplitude to the 24 hpf untreated controls shown in Fig. 3B. Following MS-222 treatment, the Ca^{2+} transients at ~25 hpf were completely absent in the CaPs (Fig. 7Ab; n=7). However, after MS-222 was washed-out, the Ca^{2+} signaling activity in the CaPs at ~26 hpf was partially restored (see arrowheads in Fig. 7Aci,Acii). In total, ~86% of the embryos (n=6) showed signs of Ca^{2+} activity recovery after the MS-222 washout. The endogenous levels of NAADP were also measured in extracts prepared from intact zebrafish embryos at ~24 hpf, which had either been untreated or else had been treated with MS-222 for 7 h starting at ~17 hpf (Fig. 7Ba). NAADP standards (Figs 7Bbi) were measured in parallel with the embryo extracts (Fig. 7Bbii) using the NAADP cycling assay (Graeff and Lee, 2013), where the read-out was the fluorescence intensity of resorufin. The results showed that the slope of the extract prepared from embryos treated with MS-222 was smaller than that of the untreated control, suggesting the presence of a lower level of NAADP after the MS-222 treatment (Fig. 7Bbii). To quantify these results, the [NAADP] measured, was normalized to the mass of protein in the embryo samples, and the fold-change in the normalized [NAADP] was calculated (Fig. 7c). Statistical analyses suggested that the [NAADP] in the MS-222-treated samples was significantly lower (by ~2-fold; at $p < 0.01$) than in the untreated controls (Fig. 7c).

DISCUSSION

It is becoming clear from a developmental perspective that TPC2 more than likely functions as a component in several integrated signaling pathways (Zhu et al., 2010; Capel et al., 2015). We attempted, therefore, to explore the contribution that TPC2-mediated Ca^{2+} release plays in a specific developmental process in an intact embryo. Our chosen embryo was that of the zebrafish, and our selected process was the initiation of the first behavioral activity that results from the establishment of early spinal cord circuitry and its integration with developing SMCs in the trunk myotome. We have not identified or characterized every molecular component of the complex signaling pathways involved in two distinct cell types, i.e., PMNs and SMCs, or indeed how all of the components of the signaling pathway interact with each other. On the other hand, we have previously reported an essential role for TPC2-mediated Ca^{2+} in the differentiation of SMCs (Kelu et al., 2015; 2017) and here we provide compelling *in vivo* evidence that TPC2-mediated Ca^{2+} release also plays a key role in PMN activity during the establishment of spontaneous SMC-mediated coilings of the trunk. Furthermore, although we do not have sufficient evidence to propose a convincing mechanistic model for the entire signaling pathway, we do propose a hypothetical model as a basis to begin further investigation. Thus, here we report a novel function of TPC2-mediated Ca^{2+} signaling during the maturation of the spinal network in zebrafish embryos. We showed that after TPC2 attenuation, the ipsilateral correlation and contralateral anti-correlation of Ca^{2+} signals in the CaPs at ~24 hpf were both repressed (Figs 1-4). It has previously been demonstrated that the spontaneous activity in the developing spinal cord of zebrafish is not affected by lesioning the hindbrain (Saint-Amant and Drapeau, 1998; 2000). This suggests that the patterned activity in the PMNs is initiated from an endogenous network in the spinal cord that is established early in development (Warp et al., 2012; Knogler et al., 2014). Recently, lysosomal/ Ca^{2+} activity has been reported to be required for the synaptic activity in rat hippocampal neurons (Padamsey et al., 2017). Our new data from zebrafish therefore add to the accumulating evidence, which suggests a role for TPC2-mediated Ca^{2+} signaling during the formation and remodeling of the neuronal circuitry. However, the mechanistic pathway that regulates the maturation of the spinal circuitry still requires further investigation.

It is clear that the phenotype seen in the SAIGFF213A;GCaMP7a double-transgenic *tpcn2*^{+/-} mutants is not as severe as that of the TPC2 morphants (Figs 1-2). This might be due to the heterozygous nature of the *tpcn2* mutation due to the SAIGFF213A;GCaMP7a double-transgenic line being crossed with the homozygous *tpcn2* mutant. It would be possible to generate an SAIGFF213A;GCaMP7a double-transgenic homozygous *tpcn2* mutant line, by incrossing pairs of SAIGFF213A;GCaMP7a heterozygous *tpcn2* mutants. However, relatively few of the homozygous *tpcn2* mutants survive to adulthood. In addition, it has been suggested that the *tpcn2*^{dhkz1a} mutation

displays an incomplete penetrance at least where its effect on the SMCs is concerned (Kelu et al., 2017). Nonetheless, the disruption of CaP Ca^{2+} signaling in the double-transgenic mutants appears to be consistent with that induced by the molecular and pharmacological attenuation of TPC2 activity (compare Figs 1-2 with Figs 3-4).

Stimulation of IP_3R -mediated Ca^{2+} release partially rescued the TPC2-knockdown phenotype of the spinal network (Fig. 5). This suggests the possibility of functional crosstalk between the acidic Ca^{2+} stores and the ER. We observed that the localization of LAMP1, TPC2 and the ER-resident IP_3R (types I and II) was similar in the primary cultures of presumptive CaPs (Fig. 6). Unfortunately, as the primary antibodies of the LAMP1/TPC2/ IP_3R (type I and type II) were all raised in the same host species (i.e., rabbit), dual-immunolabeling of any pair of these proteins was inherently difficult. Nonetheless, it has been reported that the acidic organelles and ER/SR are closely apposed in primary rat medullary neurons (Brailoiu et al., 2009) as well as in isolated rabbit ventricular cardiomyocytes (Aston et al., 2017). Studies also show that NAADP-induced Ca^{2+} release is linked to the activation of the IP_3R , and/or RyR in various neural cell preparations (Heidemann et al., 2005; Bezin et al., 2008). These reports have led to what has been termed the “trigger hypothesis”, which proposes that localized Ca^{2+} release via TPCs on the acidic stores, stimulates further Ca^{2+} release from the ER via Ca^{2+} -induced Ca^{2+} release (CICR; Galione, 2011). This hypothesis is further supported by our agonist/antagonist experiments, where treatment with the IP_3R agonist (IP_3/BM) was seen to partially rescue the Ca^{2+} signaling in the CaPs after TPC2-knockdown, and treatment with the IP_3R antagonists (2-APB or xestospongine C) disrupted both the ipsilateral and contralateral Ca^{2+} activity (Fig. S2). The function of IP_3R -mediated Ca^{2+} signaling in neurons has been studied previously (Mikoshiha, 2006; Ryglewski et al., 2007) and the subtype-specific activation of the IP_3R has also been described in different neural cell preparations (Higo et al., 2010; Perez-Alvarez et al., 2014). Hence, TPC2 in the CaPs might recruit IP_3R types I and II (but not IP_3R type III, due to the absence of labelling; Fig. 6) to amplify the Ca^{2+} signaling that is required for the coordination of the ipsilateral and contralateral activity during spinal circuit maturation.

As we could not detect any expression of RyR in the cultured CaPs with the antibodies used (Fig. 6), RyR-mediated Ca^{2+} signaling might not be involved in the regulation of the Ca^{2+} transients during the development of the spinal circuitry. Consistent with our immunolabelling results, it was previously reported that neural-specific *ryr2a* was not detected in the developing spinal cord of zebrafish embryos at ~18 hpf to ~24 hpf although its expression was observed at ~48 hpf (Wu et al., 2011). These observations are further supported by the fact that neither caffeine nor ryanodine at a low concentration (i.e., acting as RyR agonists) could rescue the inhibited Ca^{2+} signaling in the CaPs of TPC2 morphants (Fig. 5), and neither dantrolene nor ryanodine at a high concentration (i.e., acting as RyR antagonists) could block the spontaneous activity in the spinal cord (Fig. S2). Together with our

IP₃R data, this suggests the differential recruitment of the ER-Ca²⁺ channels in the functional crosstalk between the acidic Ca²⁺ stores and the ER in PMNs.

We also report that the Ca²⁺ signaling activity in the CaPs was completely inhibited and the NAADP production was reduced after the neural action potentials were blocked with MS-222 (Fig. 7). Importantly, the Ca²⁺ activity in the CaPs was reinitiated after MS-222 was washed-out. Both the amplitude and frequency of the signaling did not immediately recover to pre-treatment levels in the experimental time frame (1 h). This is usually the case in drug wash-out experiments using intact embryos (Chan et al., 2002). In our case the incomplete recovery might be due to several factors such as the time required for clearance of the drug from the fish tissue (Baron et al., 2017); the inefficient or insufficient removal of the MS-222 from the imaging chamber, as its complete removal was likely to have been hindered by the thick (i.e., ~1 to 2 mm) layer of low gelling temperature agarose, which was used to embed the embryos. In addition, full-restoration of the Ca²⁺ signaling activity of the CaPs might require a longer time (e.g., may be up to ~4 h) following MS-222 wash-out (Ramlochansingh et al., 2014).

It has recently been shown that back-propagating action potentials can stimulate Ca²⁺ release from the lysosomes in CA1 apical dendrites (Padamsey et al., 2017). It has also been reported that CD38, the mammalian homolog of ADP-ribosyl cyclase (ARC; which is the putative NAADP synthesizing enzyme), is expressed in primary mouse neurons; and application of NAADP precursors (NADP and NAAD) elicits Ca²⁺ responses in these cells (Heidemann et al., 2005). This suggests that neurons are sensitive to (and might be able to generate) NAADP (Bezin et al., 2008). Evidence for the Ca²⁺-dependent production of NAADP was provided by Vasudevan et al. (2008), who identified an NAADP synthase, which was shown to be regulated by Ca²⁺, on the surface of sea urchin sperm. The results of our NAADP cycling assay indicated the presence of endogenous levels of NAADP in embryos at ~24 hpf. However, extracts used in the assay were prepared from intact embryos, so we were not able to say with any certainty what the levels of NAADP were specifically in CaPs, or that the effects of MS-222 were specific to the CaPs. Nonetheless, the new data we present contribute to our current understanding of neural NAADP signaling by supporting the suggestion that action potentials might act as stimuli for NAADP production in neurons *in vivo*.

We report that in the CaPs, the acidic stores and TPC2 are both located in the perinuclear region in the soma as well as in clusters along the axon and at the terminal growth cone (Fig. 6B,C). The clusters of acidic stores and TPC2 within the axons (Fig. 6) might represent localized Ca²⁺ signaling hubs that regulate the establishment of possible sites of neuronal interaction, thus aiding in the transition from the sporadic and uncorrelated, to the ipsilaterally correlated and contralaterally anti-correlated activity of the early zebrafish spinal neural network (Saint-Amant and Drapeau, 2001; Warp

et al., 2012). We propose, therefore, that from ~24 hpf onwards, the basic elements of the locomotory spinal circuitry are established in developing zebrafish embryos. The early circuits then mature and develop in accordance with the locomotory and behavioral requirements of the maturing fish larvae. They start with the early spontaneous SMC-mediated trunk coilings at ~17.5 hpf, and then progress to fast muscle-mediated burst swimming in the maturing larvae (Saint-Amant and Drapeau, 1998). The new data we present suggest that TPC2-mediated Ca^{2+} release might play an important role in regulating this crucial developmental process.

In summary, we have demonstrated a pivotal role for lysosomal TPC2 channels in the generation of trains of periodic Ca^{2+} transients in CaPs and their synchronization and coordination across a network of motor neurons and the SMC of the trunk. That pharmacological inhibition of NAADP signaling phenocopies the effects of genetic knockdown and heterozygous-knockout of TPC2 expression, supports the hypothesis that TPC2 plays a key role in NAADP-mediated Ca^{2+} signaling. Our *in vivo* results help to support previous data from single cell studies where NAADP has been shown to stimulate the release of Ca^{2+} from the acidic stores via TPC2; this localized Ca^{2+} increase acts to trigger further Ca^{2+} release through the subsequent activation of IP_3Rs on the ER/SR. It has been proposed that these triggering events are likely to occur within microdomains at lysosome-ER/SR junctions (Zhu et al., 2010; Penny et al., 2015; Kelu et al., 2017; Aston et al., 2017). We propose, therefore, that TPC2 is a critical molecular component of the signaling pathway coordinating neuronal activity during the establishment of motor neuronal circuitry that controls early locomotory behavior in zebrafish.

ACKNOWLEDGEMENTS

We thank Koichi Kawakami (NIG, Japan) for providing the Gal4 and UAS transgenic lines, and Grant Churchill (University of Oxford) for teaching JJK the NAADP cycling assay.

COMPETING INTERESTS

The authors declare that they have no competing interests with the contents of this article.

FUNDING

This work was funded by the HK RGC General Research Fund awards 662113, 16101714 and 16100115, and the ANR/RGC joint research scheme award A-HKUST601/13. We also acknowledge funding from the HKITC (ITCPD/17-9), and an HKUST Overseas Research Award for JJK to work with AG. AG is a Wellcome Trust Senior Investigator.

REFERENCES

- Akerboom, J., Chen, T.W., Wardill, T.J., Tian, J., Marvin, J.S., Mutlu, S., Carreras Calderón, N., Esposti, F., Borghuis, B.G., Sun, X.R. et al. 2012. Optimization of a GCaMP calcium indicator for neural activity imaging. *J. Neurosci.* 32, 13819-13840.
- Andersen, S.L. 2002. Preparation of dissociated zebrafish spinal neuron cultures. *Meth. Cell Sci.* 23, 205-209.
- Aston, D., Capel, R.A., Ford, K.L., Christian, H.C., Mirams, G.R., Rog-Zielinska, E.A., Kohl, P., Galione, A., Burton, R.A., Terrar, D.A. 2017. High resolution structural evidence suggests the sarcoplasmic reticulum form microdomains with acidic stores (lysosomes) in the heart. *Sci. Rep.* 7: 40620 DOI: 10.1038/srep40620.
- Baron, M.G., Mintram, K.S., Owen, S.F., Hetheridge, M.J., Moody, J., Purcell, W.M., Jackson, S.K., Jha, A.N. 2017. Pharmaceutical and metabolism in fish: Using a 3-D hepatic *in vitro* model to assess clearance. *PLoS One* Doi: 10.1371/journal.pone.0168837.
- Berridge, M.J. 2012. Calcium signalling remodelling and disease. *Biochem. Soc. Trans.* 40, 297-309.
- Bezin, S., Charpentier, G., Lee, H.C., Baux, G., Fossier, P., Cancela, J.M. 2008. Regulation of nuclear Ca^{2+} signaling by translocation of the Ca^{2+} messenger synthesizing enzyme ADP-ribosyl cyclase during neuronal depolarization. *J. Biol. Chem.* 283, 27859-27870.
- Brailoiu, E., Hoard, J.L., Filipeanu, C.M., Brailoiu, G.C., Dun, S.L., Patel, S., Dun, N.J. 2005. Nicotinic acid adenine dinucleotide phosphate potentiates neurite outgrowth. *J. Biol. Chem.* 280, 5646-5650.
- Brailoiu, E., Churamani, D., Pandey, V., Brailoiu, G.C., Tuluc, F., Patel, S., Dun, N.J. 2006. Messenger-specific role for nicotinic acid adenine dinucleotide phosphate in neuronal differentiation. *J. Biol. Chem.* 281, 15923-15928.
- Brailoiu, G.C., Brailoiu, E., Parkesh, R., Galione, A., Churchill, G.C., Patel, S., Dun, N.J. 2009. NAADP-mediated channel 'chatter' in neurons of the rat medulla oblongata. *Biochem. J.* 419, 91-99.
- Brennan, C., Mangoli, M., Dyer, C.E.F., Ashworth, R. 2005. Acetylcholine and calcium signalling regulates muscle fibre formation in the zebrafish embryo. *J. Cell. Sci.* 118, 5181-5190.
- Bowman, E.J., Siebers, A., Altendorf, K. 1988. Bafilomycins: A class of inhibitors of membrane ATPases from microorganisms, animal cells, and plant cells. *Proc. Natl. Acad. Sci. USA* 85, 7972-7976.
- Calcraft, P.J., Ruas, M., Pan, Z., Cheng, X., Arredouani, A., Hao, X., Tang, J., Rietdorf, K., Teboul, L., Chuang, K.T., et al. 2009. NAADP mobilizes calcium from acidic organelles through two-pore channels. *Nature* 459, 596-600.
- Capel, R.A., Bolton, E.L., Lin, W.K., Aston, D., Wang, Y., Liu, W., Wang, X., Burton, R-A.B., Bloor-Young, D., Shade, K-T., et al. 2015. Two-pore channels (TPC2s) and nicotinic acid adenine dinucleotide

- phosphate (NAADP) at lysosomal-sarcoplasmic reticular junctions contribute to acute and chronic β -adrenoceptor signaling in the heart. *J. Biol. Chem.* 290, 30087-30098.
- Chan, J., Bayliss, P.E., Wood, J.W., Roberts, T.M. 2002. Dissection of angiogenic signaling in zebrafish using a chemical genetic approach. *Cancer Cell* 1, 257-267.
- Chen, Z., Lee, H., Henle, S.J., Cheever, T.R., Ekker, S.C., Henley, J.R. 2013. Primary neuron culture for nerve growth and axon guidance studies in zebrafish (*Danio rerio*). *PLoS One* 8, e57539.
- Cheung, C.Y., Webb, S.E., Love, D.R., Miller, A.L. 2011. Visualization, characterization and modulation of calcium signaling during the development of slow muscle cells in intact zebrafish embryos. *Int. J. Dev. Biol.* 55, 153-174.
- Dinno, A. 2015. Nonparametric pairwise multiple comparisons in independent groups using Dunn's test. *Stata J.* 15, 292-300.
- Galione, A. 2011. NAADP receptors. *Cold Spring Harb. Perspect. Biol.* 3, a004036.
- Graeff, R.M., Lee, H.C. 2013. An improved enzymatic cycling assay for NAADP. *Messenger* 2, 96-105.
- Heidemann, A.C., Schipke, C.G., Kettenmann, H. 2005. Extracellular application of nicotinic acid adenine dinucleotide phosphate induces Ca^{2+} signaling in astrocytes *in situ*. *J. Biol. Chem.* 280, 35630-35640.
- Higo, T., Hamada, K., Hisatsune, C., Nukina, N., Hashikawa, T., Hattori, M., Nakamura, T., Mikoshiba, K. 2010. Mechanism of ER stress-induced brain damage by IP_3 receptor. *Neuron* 68, 865-878.
- Hui, L., Geiger, N.H., Bloor-Young, D., Churchill, G.C., Geiger, J.D., Chen, X. 2015. Release of calcium from endolysosomes increases calcium influx through N-type calcium channels: Evidence for acidic store-operated calcium entry in neurons. *Cell Calcium* 58: 617-637.
- Jha, A., Ahuja, M., Patel, S., Brailoiu, E., Muallem, S. 2014. Convergent regulation of the lysosomal two-pore channel-2 by Mg^{2+} , NAADP, $\text{PI}(3,5)\text{P}_2$ and multiple protein kinases. *EMBO J.* 33, 501-511.
- Kelu, J.J., Chan, H.L.H., Webb, S.E., Cheng, A.H.H., Ruas, M., Parrington, J., Galione, A., Miller, A.L. 2015. Two-pore channel 2 activity is required for slow muscle cell-generated Ca^{2+} signaling during myogenesis in intact zebrafish. *Int. J. Dev. Biol.* 59, 313-325.
- Kelu, J.J., Webb, S.E., Parrington, J., Galione, A., Miller, A.L. 2017. Ca^{2+} release via two-pore channel type 2 (TPC2) is required for slow muscle cell myofibrillogenesis and myotomal patterning in intact zebrafish embryos. *Dev. Biol.* 425, 109-129.
- Knogler, L.D., Ryan, J., Saint-Amant, L., Drapeau, P. 2014. A hybrid electrical/chemical circuit in the spinal cord generates a transient embryonic motor behavior. *J. Neurosci.* 34, 9644-9655.
- Meissner, G. 1986. Ryanodine activation and inhibition of the Ca^{2+} release channel of sarcoplasmic reticulum. *J. Biol. Chem.* 261, 6300-6306.

- Melançon, E., Liu, D.W.C., Westerfield, M., Eisen, J.S. 1997. Pathfinding by identified zebrafish motoneurons in the absence of muscle pioneers. *J. Neurosci.* 17, 7796-7804.
- Mikoshiba, K. 2006. Inositol 1, 4, 5-trisphosphate (IP₃) receptors and their role in neuronal cell function. *J. Neurochem.* 97, 1627-1633.
- Muto, A., Ohkura, M., Kotani, T., Higashijima, S.I., Nakai, J., Kawakami, K. 2011. Genetic visualization with an improved GCaMP calcium indicator reveals spatiotemporal activation of the spinal motor neurons in zebrafish. *Proc. Natl. Acad. Sci. USA* 108, 5425-5430.
- Naganawa, Y., Hirata, H. 2011. Developmental transition of touch response from slow muscle-mediated coilings to fast muscle-mediated burst swimming in zebrafish. *Dev. Biol.* 355, 194-204.
- Naylor, E., Arredouani, A., Vasudevan, S.R., Lewis, A.M., Parkesh, R., Mizote, A., Rosen, D., Thomas, J.M., Izumi, M., Ganesan, A., et al. 2009. Identification of a chemical probe for NAADP by virtual screening. *Nat. Chem. Biol.* 5, 220-226.
- Padamsey, Z., McGuinness, L., Bardo, S.J., Reinhart, M., Tong, R., Hedegaard, A., Hart, M.L., Emptage, N.J. 2017. Activity-dependent exocytosis of lysosomes regulates the structural plasticity of dendritic spines. *Neuron* 93, 132-146.
- Penny, C.J., Kilpatrick, B.S., Eden, E.R., and Patel, S. (2015). Coupling acidic organelles with the ER through Ca²⁺ microdomains at membrane contact sites. *Cell Calcium* 58, 387-396.
- Perez-Alvarez, A., Navarrete, M., Covelo, A., Martin, E.D., Araque, A. 2014. Structural and functional plasticity of astrocyte processes and dendritic spine interactions. *J. Neurosci.* 34, 12738-12744.
- Plazas, P.V., Nicol, X., Spitzer, N.C. 2013. Activity-dependent competition regulates motor neuron axon pathfinding via plexinA3. *Proc. Natl. Acad. Sci. USA.* 110, 1524-1529.
- Ramlochansingh, C., Branoner, F., Chagnaud, B.P. and Straka, H. 2014. Efficacy of tricaine methanesulfonate (MS-222) as an anesthetic agent for blocking sensory-motor responses in *Xenopus laevis* tadpoles. *PLoS One* 9, e101606.
- Rizzuto, R., De Stefani, D., Raffaello, A., Mammucari, C. 2012. Mitochondria as sensors and regulators of calcium signaling. *Nature Rev. Mol. Cell Biol.* 13, 566-578.
- Rosenberg, S.S., Spitzer, N.C. 2011. Calcium signaling in neuronal development. *Cold Spring Harb. Perspect. Biol.* 3, a004259.
- Ryglewski, S., Pflueger, H.J., Duch, C. 2007. Expanding the neuron's calcium signaling repertoire: intracellular calcium release via voltage-induced PLC and IP₃R activation. *PLoS Biol.* 5, e66.
- Ruas, M., Davis, L.C., Chen, C.C., Morgan, A.J., Chuang, K.T., Walseth, T.F., Grimm, C., Garnham, C., Powell, T., Platt, N. et al. 2015. Expression of Ca²⁺-permeable two-pore channels rescues NAADP signalling in TPC-deficient cells. *EMBO J.* 34, 1743-1758

- Saint-Amant, L., Drapeau, P. 1998. Time course of the development of motor behaviors in the zebrafish embryo. *J. Neurobiol.* 37, 622-32.
- Saint-Amant, L., Drapeau, P. 2000. Motoneuron activity patterns related to the earliest behavior of the zebrafish embryo. *J. Neurosci.* 20, 3964-3972.
- Saint-Amant, L., Drapeau, P. 2001. Synchronization of an embryonic network of identified spinal interneurons solely by electrical coupling. *Neuron* 31, 1035-1046.
- Vasudevan, S.R., Galione, A., Churchill, G.C. 2008. Sperm express a Ca^{2+} -regulated NAADP synthase. *Biochem. J.* 411, 63-70.
- Warp, E., Agarwal, G., Wyart, C., Friedmann, D., Oldfield, C.S., Conner, A., Del Bene, F., Arrenberg, A.B., Baier, H., Isacoff, E.Y. 2012. Emergence of patterned activity in the developing zebrafish spinal cord. *Curr. Biol.* 22, 93-102.
- Westerfield, M. 2000. *The Zebrafish Book: A guide for the laboratory use of zebrafish (Danio rerio)* Oregon, USA: University of Oregon Press.
- Wilson, S.W., Brand, M., Eisen, J.S. 2002. Patterning the zebrafish central nervous system. In: *Pattern Formation in Zebrafish. Results and Problems in Cell Differentiation* (ed. Solnica-Krezel L.) vol 40. pp. 181-215. Berlin, Heidelberg: Springer.
- Wu, H.H., Brennan, C., Ashworth, R. 2011. Ryanodine receptors, a family of intracellular calcium ion channels, are expressed throughout early vertebrate development. *BMC Res. Notes* 4, 541.
- Zhang, Z.H., Lu, Y.Y., Yue, J. 2013. Two pore channel 2 differentially modulates neural differentiation of mouse embryonic stem cells. *PLoS One* 8, e66077.
- Zhu, M.X., Evans, A.M., Ma, J., Parrington, J., Galione, A. 2010. Two-pore channels for integrative Ca^{2+} signaling. *Comm. Int. Biol.* 3: 12-17.

FIGURE LEGENDS

Fig. 1. Effect of TPC2-knockdown, heterozygous-knockout, and mRNA rescue on the spontaneous Ca^{2+} activity of the CaPs in SAIGFF213A;UAS:GCaMP7a embryos at ~24 hpf. SAIGFF213A;UAS:GCaMP7a embryos were injected with: (A) Standard control-MO; (B) *p53*-MO; (C) *TPCN2*-MO-T with *p53*-MO; or (D) *TPCN2*-MO-T with *p53*-MO and the mutant *tpcn2*-mRNA. In addition, (E) untreated SAIGFF213A;UAS:GCaMP7a fish (termed *tpcn2*^{+/+} controls) were imaged and (F) they were crossed with homozygous *tpcn2*^{dhkz1a} mutants to generate double-transgenic heterozygous mutants (*tpcn2*^{+/-}). (Ai-Fiv) Time-lapse fluorescence images showing the changes in GCaMP7a fluorescence in the CaPs at different time intervals in the various treatment groups. The embryos are in a dorsal orientation and regions of interest (ROIs) on two (of the three) selected CaP cell bodies on the left (L) and right (R) sides of the spinal cord are shown. The arrowheads indicate GCaMP7a signals in the CaPs. Ant. and Pos. are anterior and posterior, respectively. Scale bar, 50 μm . (Av-Fv) Line graphs showing the $\Delta F/F_0$ against time (over a period of ~300 sec) in the ROIs of the representative embryos shown in (Ai-Fiv), respectively. The time period that corresponds to the Ca^{2+} signaling events shown in the time-lapse fluorescence images (Ai-Fiv) is denoted by a grey vertical bar in (Av-Fvi). Also see Movies S1-S3, which illustrate the distinct right/left alternation of Ca^{2+} transients in the controls and how this is disrupted when TPC2-mediated Ca^{2+} release was inhibited.

Fig. 2. Analysis of the effect of TPC2-knockdown, heterozygous-knockout, and mRNA rescue on the spontaneous Ca^{2+} activity of the CaPs in SAIGFF213A;UAS:GCaMP7a embryos at ~24 hpf. (A) Cross correlograms to compare the Ca^{2+} activity in the (Aai-Afi) ipsilateral (same side) and (Aaii-Afii) contralateral (opposite side) CaPs in the various treatment groups shown in Fig. 1. The cross correlation function (CCF) at lag ± 1.5 sec is shown. (B) Bar graphs to show the mean \pm SEM CCF at the zero-lag (CCF0) of the (Ba) ipsilateral and (Bb) contralateral CaP Ca^{2+} activity. (C-E) Bar graphs to show the mean \pm SEM (C) frequency and (D) amplitude, and (E) duration of the Ca^{2+} transients in the CaPs of the double-transgenic embryos in the various treatment groups. Data were obtained from n=30-72 cells from 5-8 embryos, except for the duration data, which were n=6 from 3 embryos. $p < 0.05$ (*), $p < 0.01$ (**) and $p < 0.001$ (***), and NS indicates no significant difference between the data.

Fig. 3. Effect of depleting the acidic Ca^{2+} stores and antagonizing TPCs on the spontaneous Ca^{2+} activity of the CaPs in SAIGFF213A;UAS:GCaMP7a embryos at ~18 hpf and ~24 hpf. Embryos were (A,B) untreated, or (C-H) they were treated with: (C,D) 1% DMSO, (E,F) 1 μM bafilomycin A1, or (G,H) 250 μM *trans*-Ned-19. Drug treatments started at ~17 hpf, and finished at either (A,C,E,G) ~18 hpf or

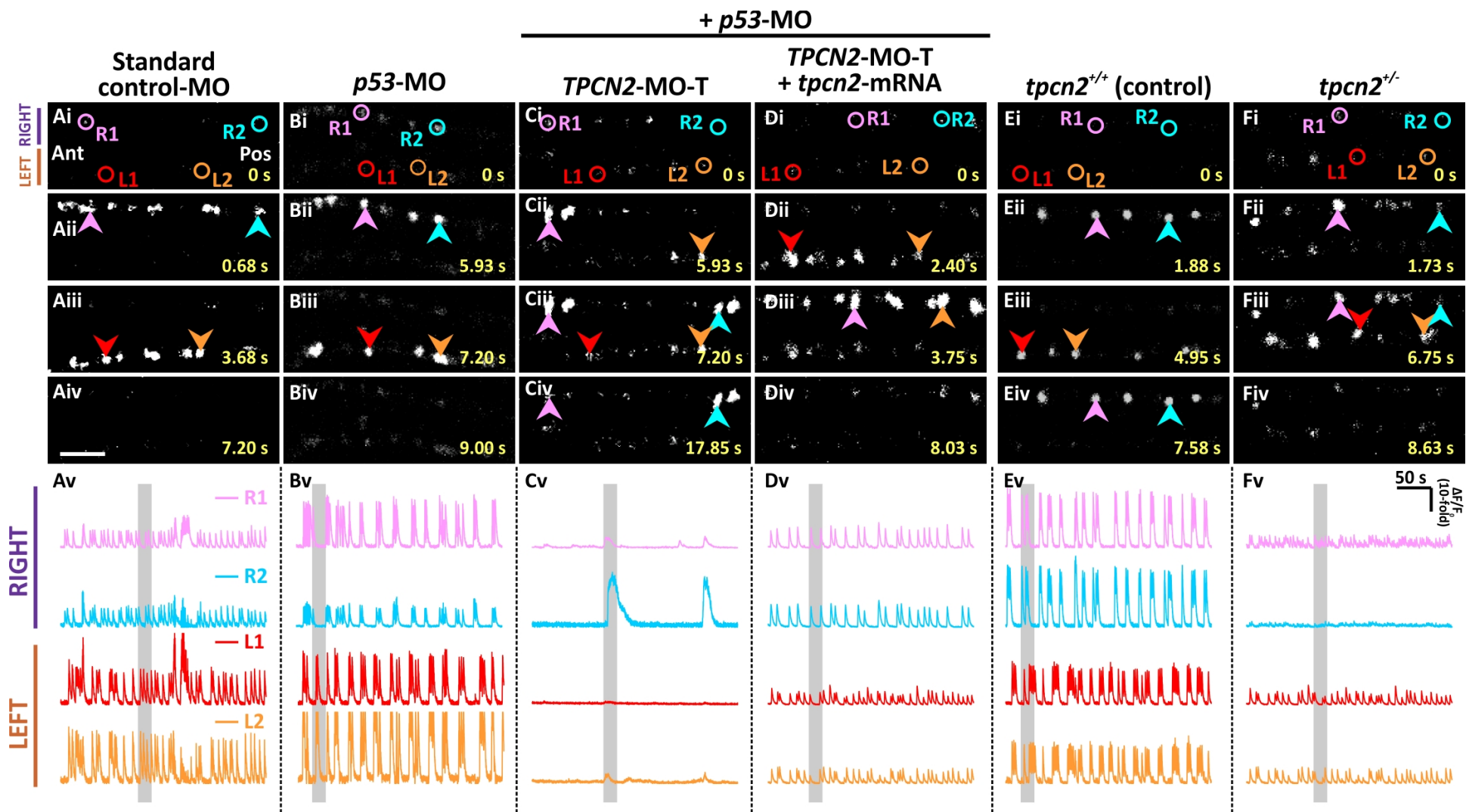
(B,D,F,H) ~24 hpf. (Ai-Hiv) Time-lapse fluorescence images, and (Av-Hv) line graphs as described in Fig.1.

Fig. 4. Analysis of the effect of depleting the acidic Ca^{2+} stores and antagonizing TPCs on the spontaneous Ca^{2+} activity of the CaPs in SAIGFF213A;UAS:GCaMP7a embryos at ~18 hpf and ~24 hpf. (A) Bar graphs to show the mean \pm SEM cross correlation function at zero-lag of the (Aa) ipsilateral, and (Ab) contralateral CaP Ca^{2+} activity. (B-D) Bar graphs to show the mean \pm SEM (B) frequency, (C) amplitude and (D) duration of the Ca^{2+} spikes in the CaPs of the double-transgenic embryos in the various treatment groups. For both ~18 hpf and ~24 hpf, data were obtained from n=18-63 cells from 3-7 embryos, except for the duration data, which were n=6 cells from 3 embryos. $p < 0.01$ (**), and $p < 0.001$ (***), and NS indicates no significant difference between the data.

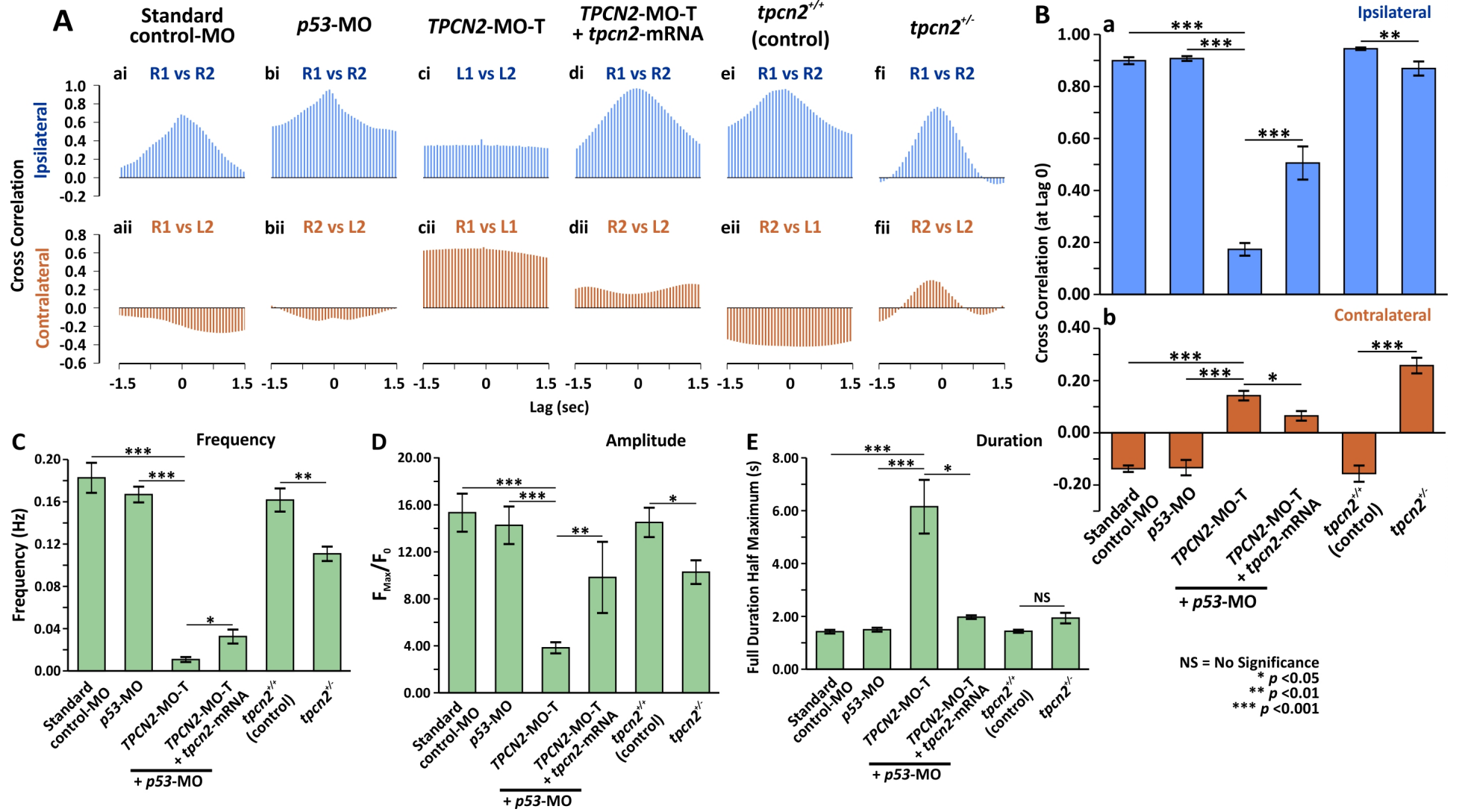
Fig. 5. Effect of stimulating the ER-mediated Ca^{2+} release on the spontaneous Ca^{2+} activity of the CaPs in SAIGFF213A;UAS:GCaMP7a embryos at ~24 hpf after MO-based TPC2-knockdown. Embryos that had been injected with TPCN2-MO-T at the 1- to 4-cell stage to knockdown TPC2, were treated with: (Aa) 1% DMSO; (Ab) 100 μM IP_3 /BM; (Ac) 2 mM caffeine; or (Ad) 1 μM ryanodine at ~17 hpf. (Aai-Adv) Time-lapse fluorescence images, and (Aav-Adv) line graphs as described in Fig. 1. (B) Bar graphs to show the mean \pm SEM cross correlation function at zero-lag of the (Ba) ipsilateral, and (Bb) contralateral CaP Ca^{2+} activity. (C-E) Bar graphs to show the mean \pm SEM (C) frequency, (D) amplitude and (E) duration of the Ca^{2+} spikes in the CaPs of the embryos in the various treatment groups. Data were obtained from n=30-90 cells from 5-10 embryos, except for the duration data, which were n=6 cells from 3 embryos. $p < 0.01$ (**), and $p < 0.001$ (***), and NS indicates no significant difference between the data.

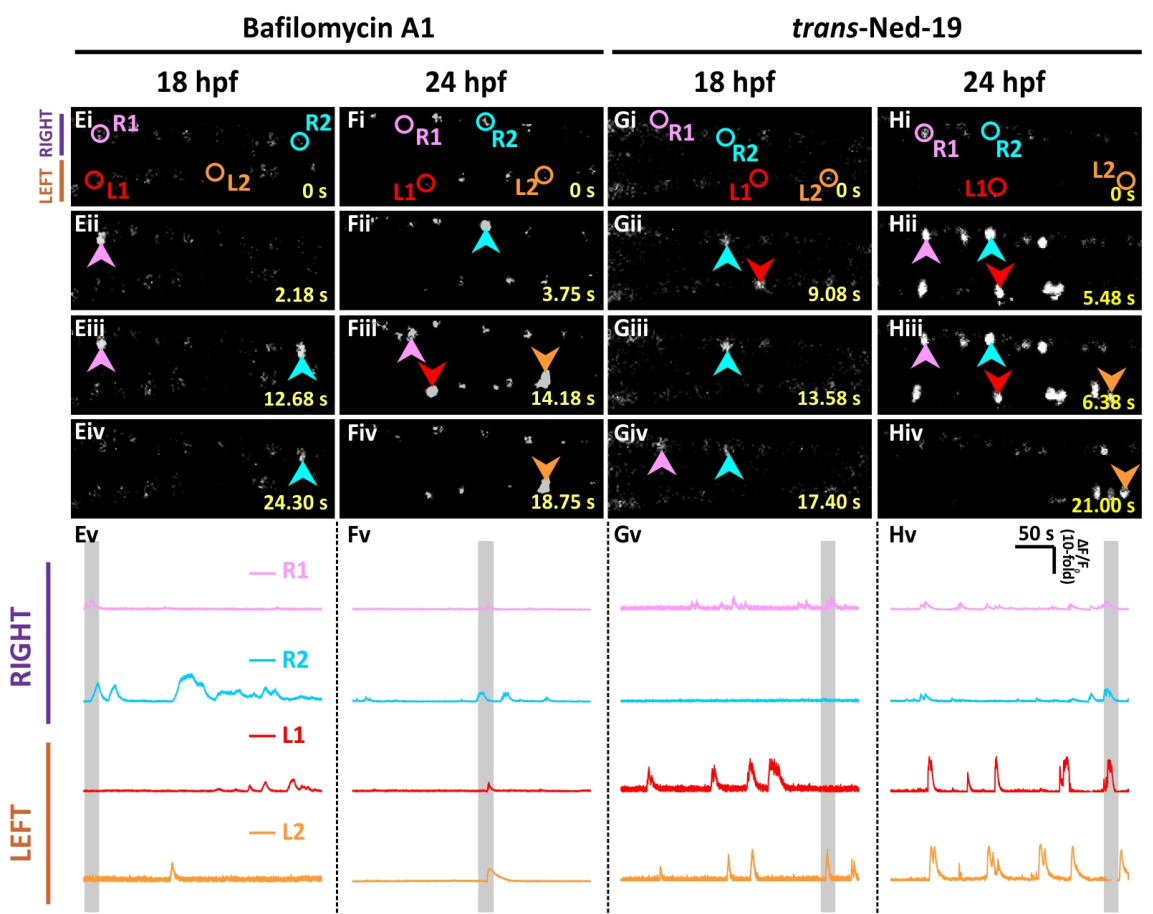
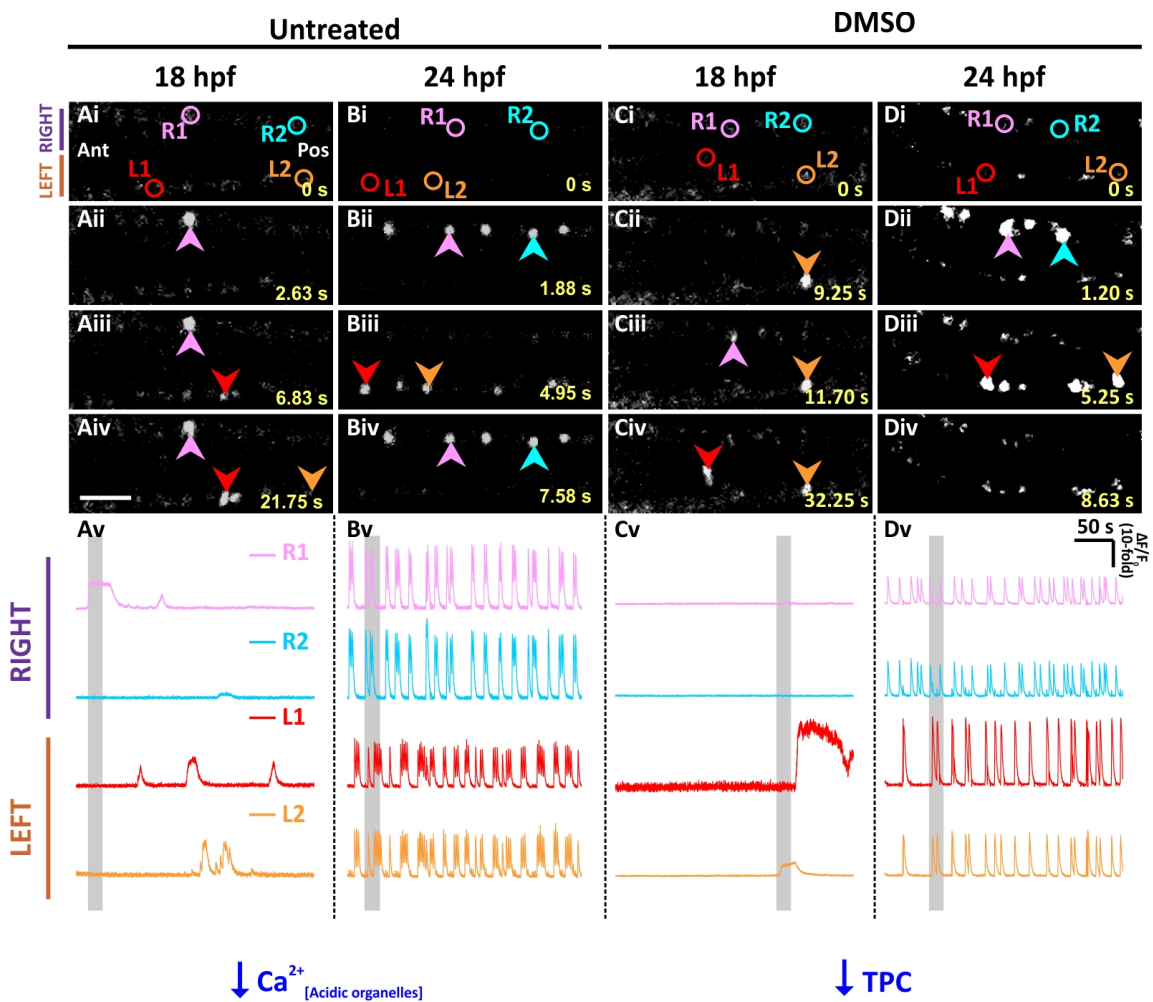
Fig. 6. Expression and localization of LAMP1, TPC2, IP_3 R and RyRs in presumptive CaPs isolated from SAIGFF213A;UAS:GFP embryos and cultured for 24 hr. The trunk of these embryos, which (Ai-Hi) express GFP in the CaPs, was dissected at ~18 hpf. The cells were dissociated and cultured for 24 hr and then they were immunolabelled with antibodies for (Aii) PMNs, (Bii) lysosomal-associated membrane protein 1 (LAMP1), (Cii) TPC2, (Dii-Fii) IP_3 R types I-III, respectively, or (Gii) RyR (all subtypes). Panel (Hii) shows a secondary antibody control. (Aiii-Hiii) The cells were co-stained with DAPI to label the nuclei. Each panel is a series of optical sections that have been projected as a single confocal image, and they show: (Ai-Hi) GFP in the presumptive CaPs (in green); (Aii-Hii) the localization of the various proteins immunolabelled (in red); (Aiii-Hiii) the DAPI-labeled nuclei (in blue); and (Aiv-Hiv) images showing the red and blue channels when merged. Scale bars, 10 μm .

Fig. 7. Effect of inhibiting the action potentials on the spontaneous Ca^{2+} activity of the CaP in SAIGFF213A;UAS:GCaMP7a embryos, and on the production of NAADP by AB wild-type embryos, at ~24 hpf. SAIGFF213A;UAS:GCaMP7a embryos were (Aa) imaged at ~24 hpf. (Ab) MS-222 was then applied for 1 h and the embryos were imaged again (i.e., at ~25 hpf). (Ac) Subsequently, the MS-222-treated embryos were washed with Danieau's solution for 1 h, after which they were imaged one more time (i.e., at ~26 hpf). (Aai-Aciv) Time-lapse fluorescence images, and (Aav-Acv) line graphs as described in Fig. 1. The data presented in panels Aa-Ac were collected from the same representative embryo. (Ad) schematic to show the timing of the MS-222 treatment and washout experiments. (B) The NAADP cycling assay was used to detect the endogenous level of NAADP in embryos at ~24 hpf. (Ba) Schematic to show the timing of the MS-222 treatment. (Bb) Line graphs show the change in the fluorescence intensity of resofurin over time (covering a period of ~270 min) such that (Bbi) shows NAADP standards of 0 nM to 40 nM, and (Bbii) shows NAADP measured in samples prepared from intact embryos at ~24 hpf in the absence/ presence of MS-222. These plots were then fitted into linear regression models, and the slope (m) of fluorescence increase was determined by $y=mx+c$. (Bc) Bar graph showing the normalized [NAADP], and the corresponding fold-change of [NAADP] in the samples prepared from embryos \pm MS-222 (n=9 from 3 independent assays). $p<0.01$ (**).



+ p53-MO

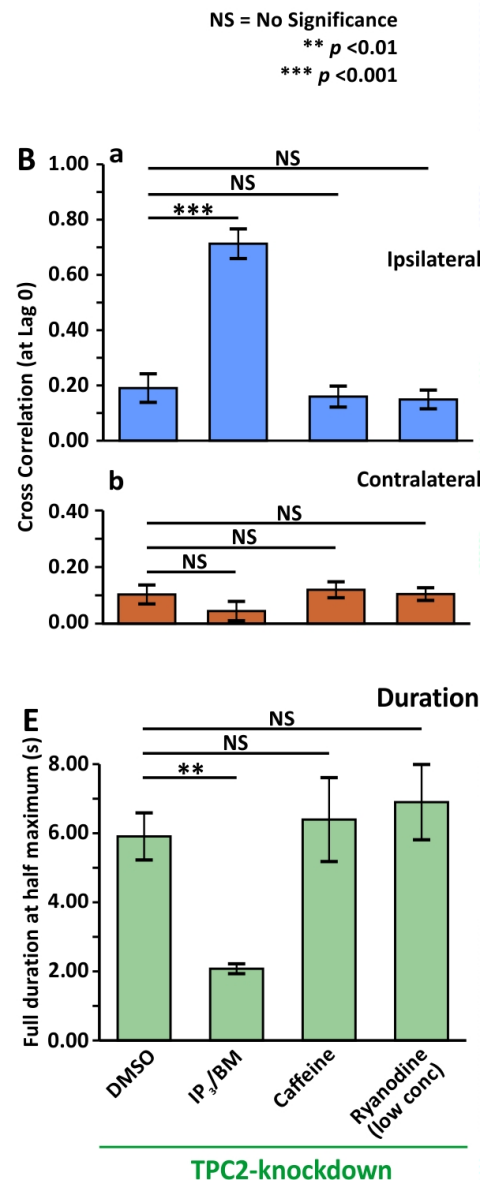
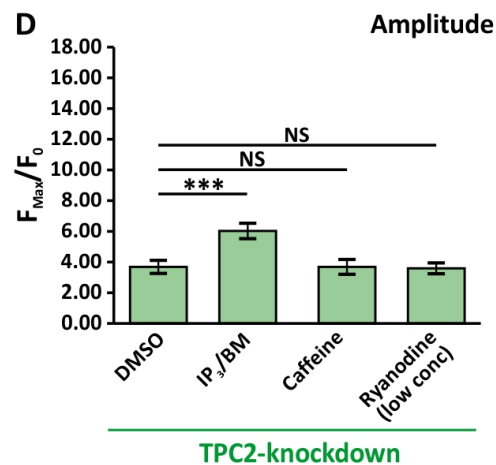
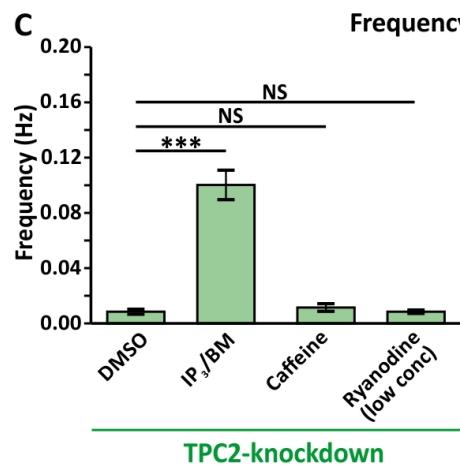
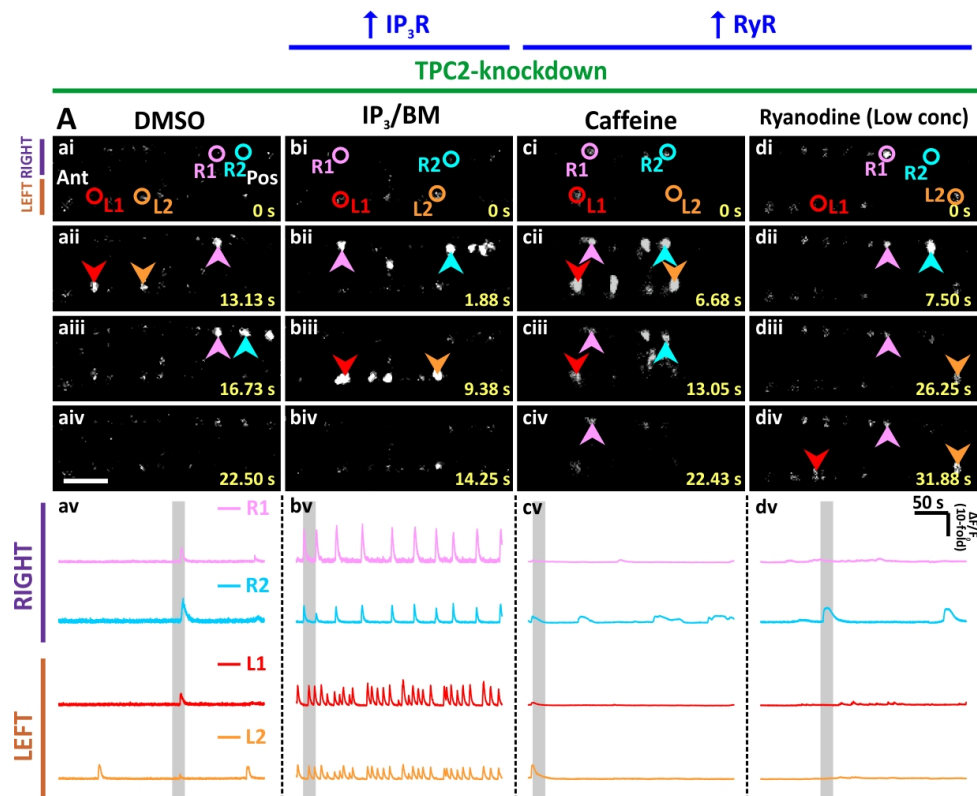


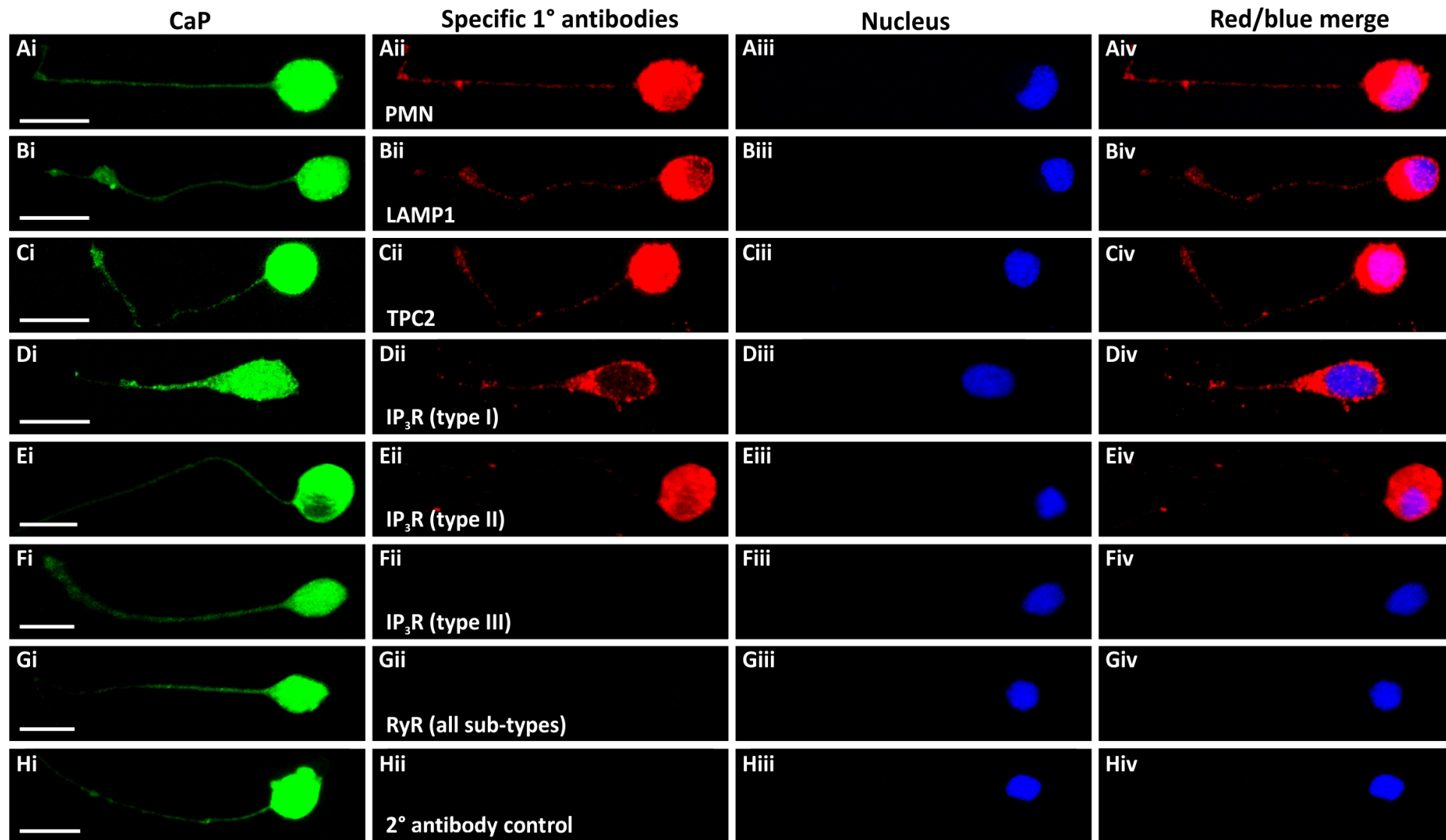




*** $p < 0.001$

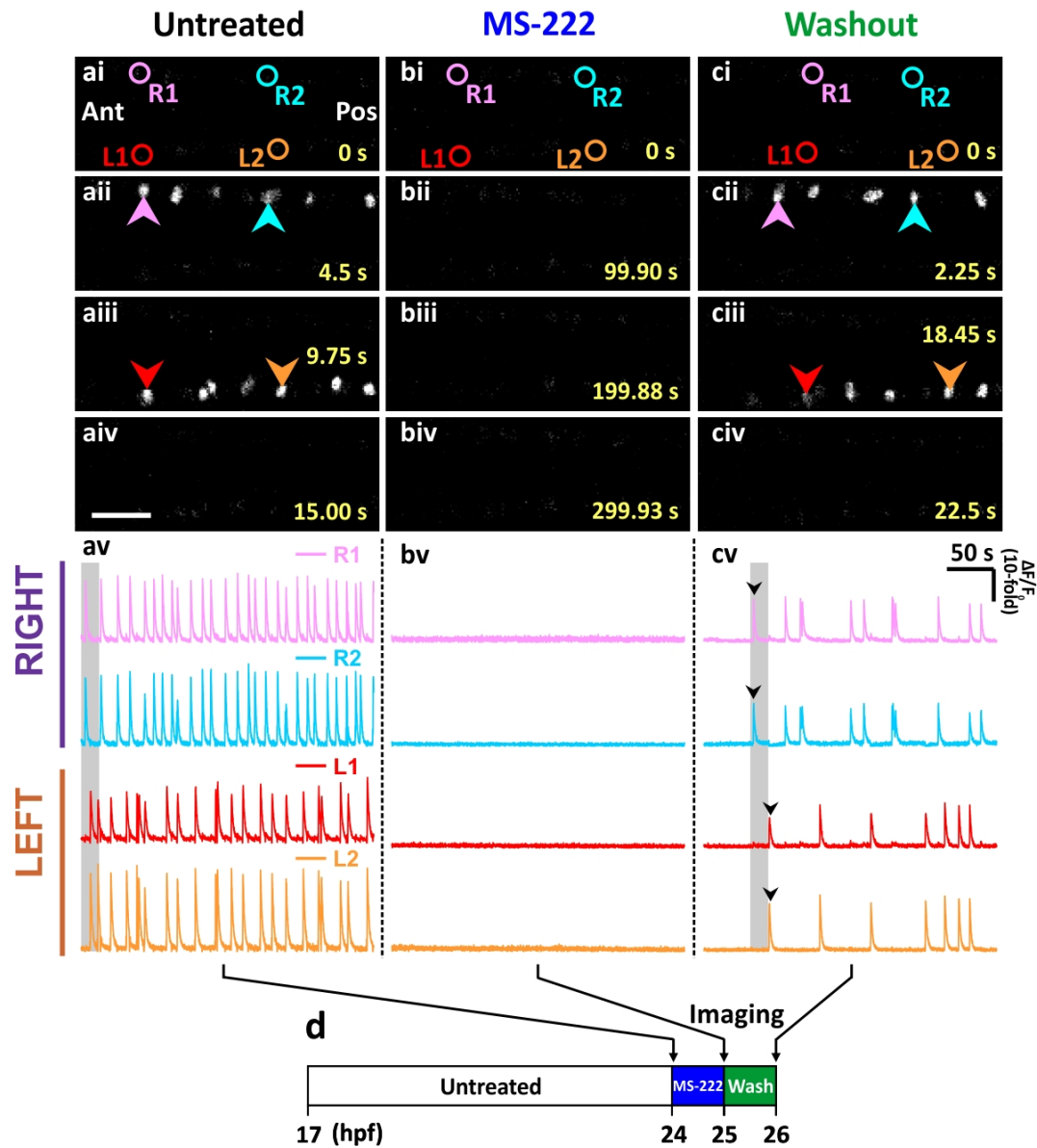




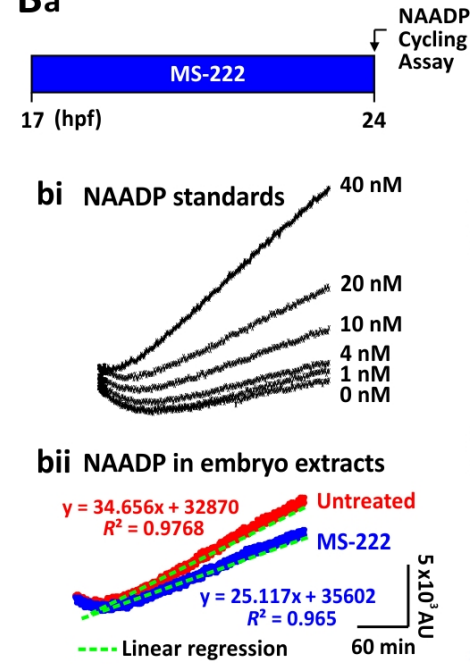


A

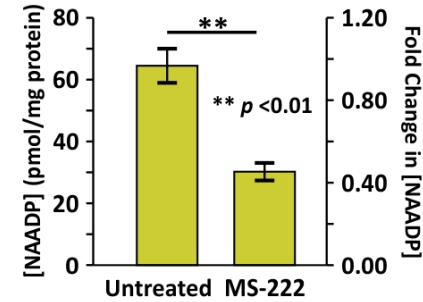
Scheme 1



Ba



c



SUPPLEMENTARY INFORMATION

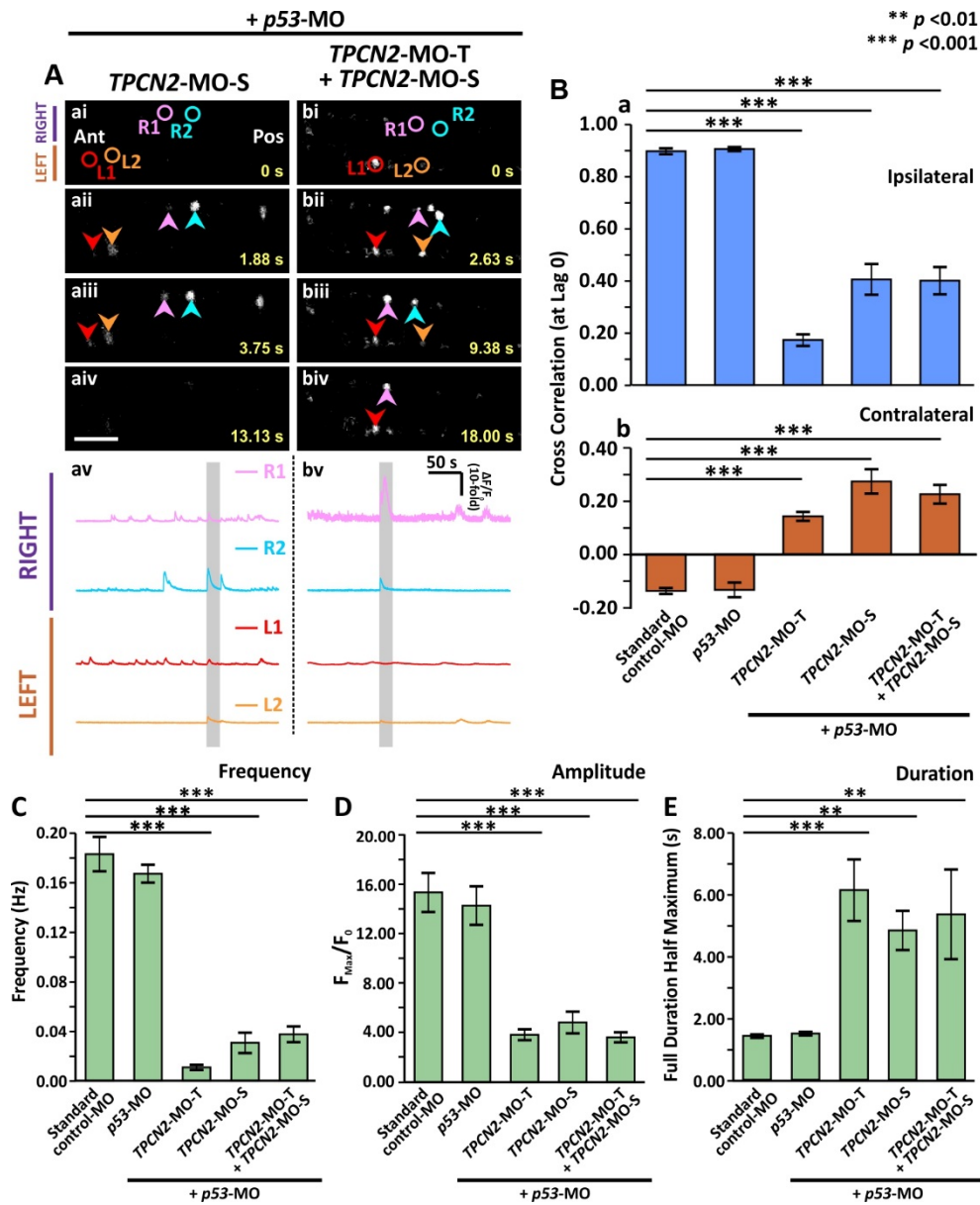


Fig. S1. Effect of MO-based knockdown of TPC2 (via injection of either *TPCN2-MO-S* or *TPCN2-MO-S* and *TPCN2-MO-T*) on the spontaneous Ca^{2+} activity of CaPs in SAIGFF213A;UAS:GCaMP7a double-transgenic embryos at ~24 hpf. SAIGFF213A;UAS:GCaMP7a embryos were injected with: (Aa) *TPCN2-MO-S* with *p53-MO*; or (Ab) *TPCN2-MO-T* and *TPCN2-MO-S* with *p53-MO*. (Aai-Abiv) Time-lapse fluorescence images showing the changes in GCaMP7a fluorescence in the CaPs at different time intervals in the two treatment groups. The embryos are in a dorsal orientation and regions of interest (ROIs) on two selected CaP cell bodies on the left (L) and right (R) sides of the spinal cord are shown. The arrowheads indicate GCaMP7a signals in the CaPs. Ant. and Pos. are anterior and posterior, respectively. Scale bar is 50 μm . (Aav,Abv) Line graphs to show the $\Delta F/F_0$ against time (over a period of ~300 sec) in the ROIs

of the representative embryos shown in (Aai-Abiv), respectively. The time period that corresponds to the Ca^{2+} signaling events shown in the time-lapse fluorescence images (Aai-Abiv) is denoted by a grey vertical bar in (Aav-Abvi). (B) Bar graphs to show the mean \pm SEM cross correlation function at zero lag of the (Ba) ipsilateral, and (Bb) contralateral CaP Ca^{2+} activity. (C-E) Bar graphs to show the mean \pm SEM (C) frequency, (D) amplitude and (E) duration of the Ca^{2+} spikes in the CaPs of the double-transgenic embryos in the various treatment groups. Data were obtained from n=24-63 cells from 4-7 embryos, except for the duration data, which were n=6 cells from 3 embryos. $p < 0.01$ (**), and $p < 0.001$ (***), and NS indicates no significant difference between the data.

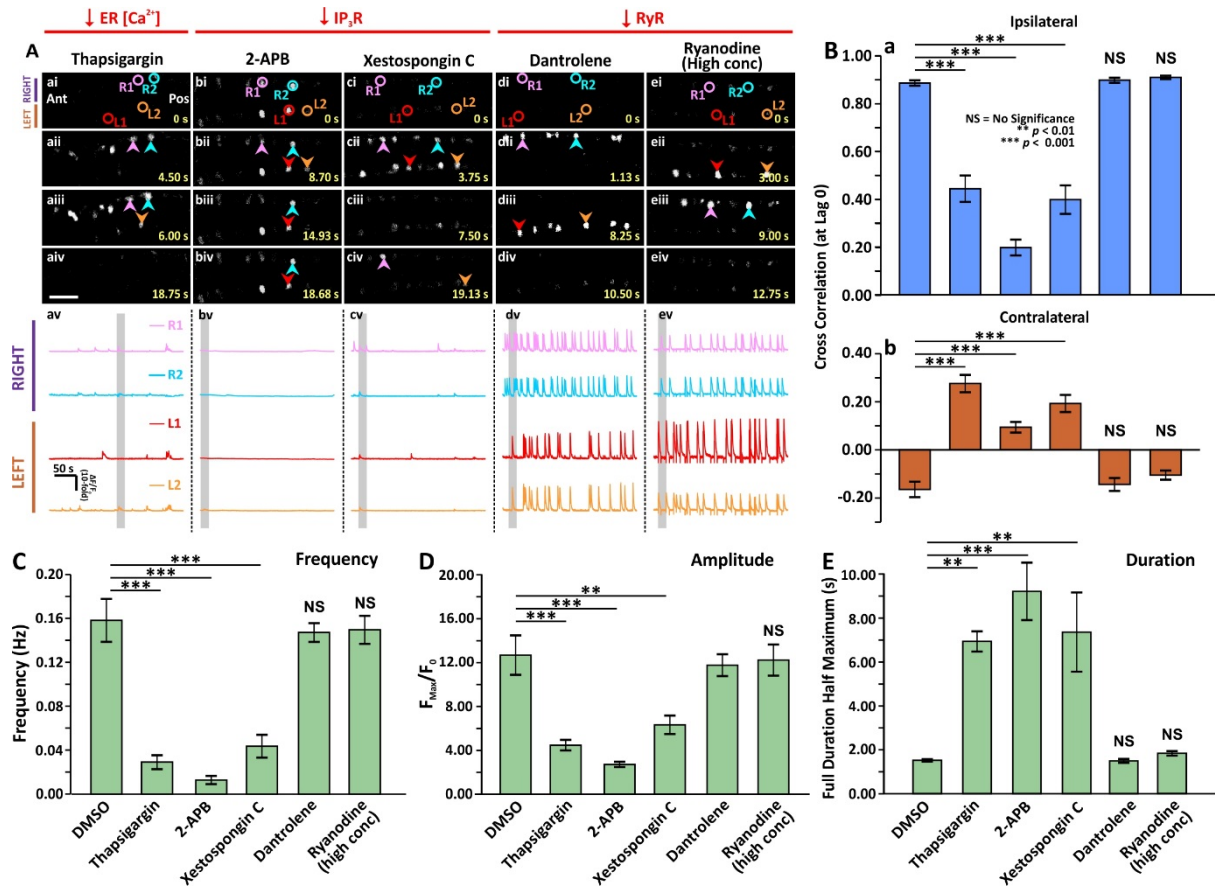


Fig. S2. Effect of thapsigargin, 2-APB, xestospongine C, dantrolene or ryanodine (at a high concentration) on the spontaneous Ca²⁺ activity of CaPs in SAIGFF213A;UAS:GCaMP7a double-transgenic embryos. SAIGFF213A;UAS:GCaMP7a embryos were treated with: (Aa) 1 μ M thapsigargin; (Ab) 10 μ M 2-APB; (Ac) 1 μ M xestospongine C; (Ad) 50 μ M dantrolene, or (Ae) 50 μ M ryanodine at 17 hpf via tail-bud excision. (Aai-Aeiv) Time-lapse fluorescence images showing the changes of GCaMP7a fluorescence signals in the CaPs at different time intervals in the various treatment groups. The embryos are in a dorsal orientation and ROIs on two selected CaP cell bodies on the left (L) and right (R) sides of the spinal cord are shown. The arrowheads indicate the increase in GCaMP7a signals in the CaPs. Ant. and Pos. are anterior and posterior, respectively. Scale bar is 50 μ m. (Aav-Aev) Line graphs to show the $\Delta F/F_0$ against time (over a period of ~300 sec) in the ROIs of the representative embryos shown in (Aai-Aeiv), respectively. The time period that corresponds to the Ca²⁺ signaling events shown in the time-lapse fluorescence images (Aai-Aeiv) is denoted by a grey vertical bar in (Aav-Aevi). (B) Bar graphs to show the mean \pm SEM cross correlation at zero lag of the (Ba) ipsilateral, and (Bb) contralateral CaP Ca²⁺ activity. (C-E) Bar graphs to show the mean \pm SEM (C) frequency, (D) amplitude and (E) duration of the Ca²⁺ spikes in the CaPs of the double-transgenic embryos in the various treatment groups. Data were obtained from n=18-81 cells from 3-9 embryos, except for the duration data, which were n=6

cells from 3 embryos. $p < 0.01$ (**) and $p < 0.001$ (***), and NS indicates no significant difference between the data.

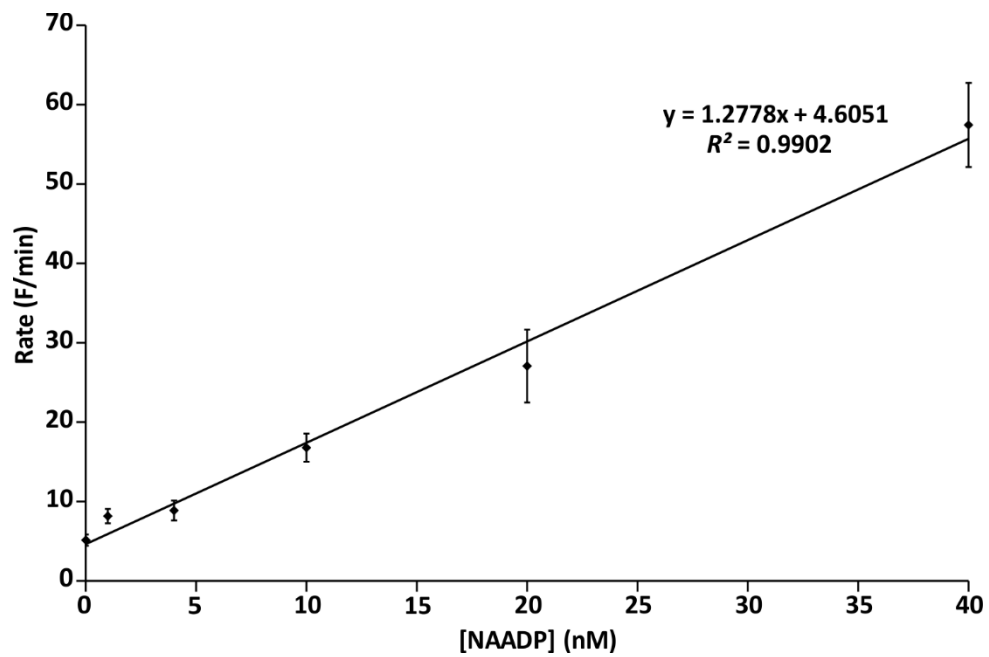


Fig. S3. Representative NAADP standard curve obtained from the NAADP cycling assay. The reaction rate (i.e., the change in resorufin fluorescence over time), was plotted against [NAADP] (n=3 for each concentration) and then fitted into a linear regression model.

Supplemental Movies

Movie 1. Time-lapse fluorescence imaging to show the spontaneous Ca^{2+} activity in the CaPs of a representative SAIGFF213A;UAS:GCaMP7a embryo at ~24 hpf during normal development. Embryos were injected with *p53*-MO alone at the one-cell stage. Images were collected every 0.075 ms for 5 min, and the video was speeded up 30 times to show the GCaMP7a fluorescence in the CaP cell bodies. The embryo is in a dorsal orientation and anterior is to the left. Scale bar, 50 μm .

Movie 2. Time-lapse fluorescence imaging to show the effect of TPC2-knockdown on the spontaneous Ca^{2+} activity in the CaPs of a representative SAIGFF213A;UAS:GCaMP7a embryo at ~24 hpf. Embryos were injected with *TPCN2*-MO-T and *p53*-MO at the one-cell stage. Images were collected every 0.075 ms for 5 min, and the video was speeded up 30 times to show the GCaMP7a fluorescence in the CaP cell bodies. The embryo is in a dorsal orientation and anterior is to the left. Scale bar, 50 μm .

Movie 3. Time-lapse fluorescence imaging to show the effect of TPC2-knockdown and mRNA rescue on the spontaneous Ca^{2+} activity of a representative SAIGFF213A;UAS:GCaMP7a embryo at ~24 hpf. Embryos were co-injected with *TPCN2*-MO-T, *p53*-MO and the mutant *tpcn2* mRNA at the one-cell stage. Images were collected every 0.075 ms for 5 min, and the video was speeded up 30 times to show the GCaMP7a fluorescence in the CaP cell bodies. The embryo is in a dorsal orientation and anterior is to the left. Scale bar, 50 μm .

Supplemental Experimental Procedures

Design and injection of morpholino (MO) oligomers and mRNA rescue construct

The TPCN2-MO-S was designed, prepared and injected into embryos, as previously described (Kelu et al., 2015, 2017).

Pharmacological treatments

Stock solutions of thapsigargin, 2-aminoethoxydiphenyl borate (2-APB), xestospongine C, and dantrolene were prepared in DMSO at 500 μ M, 5 mM, 100 μ M, and 10 mM, respectively, whereas a stock of ryanodine was prepared in Milli-Q water at 5 mM. All of these pharmacological agents were from Sigma-Aldrich Corp., apart from xestospongine C, which was from Tocris Bioscience. Thapsigargin was used at 1 μ M; 2-APB and xestospongine C were used at 10 μ M and 1 μ M, respectively; and dantrolene and ryanodine were both used at 50 μ M. All the drugs were kept at -20°C in aliquots, and then thawed and diluted to the respective working concentration in Danieau's solution just prior to the start of the incubation (Kelu et al., 2015, 2017).

References

- Kelu, J.J., Chan, H.L.H., Webb, S.E., Cheng, A.H.H., Ruas, M., Parrington, J., Galione, A., Miller, A.L. 2015. Two-pore channel 2 activity is required for slow muscle cell-generated Ca^{2+} signaling during myogenesis in intact zebrafish. *Int. J. Dev. Biol.* 59, 313-325.
- Kelu, J.J., Webb, S.E., Parrington, J., Galione, A., Miller, A.L. 2017. Ca^{2+} release via two-pore channel type 2 (TPC2) is required for slow muscle cell myofibrillogenesis and myotomal patterning in intact zebrafish embryos. *Dev. Biol.* 425, 109-129.